2022-08-08

Considerations for and Development of Sound Level Maps for the M16A4 Rifle

Reese D. Rasband
Brigham Young University

Considerations for and Development of

Sound Level Maps for the M16A4 Rifle

Reese D. Rasband

A thesis submitted to the faculty of
Brigham Young University
in partial fulfillment of the requirements for the degree of

Master of Science

Kent L. Gee, Chair
Brian E. Anderson
Timothy W. Leishman

Department of Physics and Astronomy

Brigham Young University

ABSTRACT

Considerations for and Development of
Level Maps for the M16A4 Rifle

Reese D. Rasband
Department of Physics and Astronomy, BYU
Master of Science

Considerations for and Development of Sound Level Maps for the M16A4 Rifle - REESE D. RASBAND, Department of Physics & Astronomy, Brigham Young University, Provo, UT 84602, KENT L. GEE, Department of Physics & Astronomy, Brigham Young University, Provo, UT 84602, BRIAN E. ANDERSON, Department of Physics & Astronomy, Brigham Young University, Provo, UT 84602, TIMOTHY W. LEISHMAN, Department of Physics & Astronomy, Brigham Young University, Provo, UT 84602 ---

Small firearms can create sound levels exceeding the safe threshold of human hearing with even one shot. Understanding how the sound propagates will lead to better range and military drill design. This thesis describes errors associated with different predictive interpolation models for the M16A4. Before directly discussing potential sources of error, the thesis first seeks to validate the data acquired. This is done through waveform inspection with a focus on shot-to-shot consistency. Finding the standard deviation in level between a 10-shot volley provides a good baseline with which other sources of error can be compared to. For both peak and 8-hour A-weighted equivalent levels, the deviation tended to be 1-1.2 dB. With this constraint in mind, the thesis then discussions potential error of measurements along the radial arc. By comparing nearest neighbor microphones with measured values, it was determined that a finer resolution behind the shooter is most relevant. Second, radial propagation was plotted to justify potential decay rates for further plotting. A model of spherical spreading is reasonable, but overestimates the level at farther distances e.g. 50 m. Lastly the thesis focuses on interpolation mapping to predict levels around the range. The baseline model was created using a Cartesian interpolation scheme that uses ghost points to help limit potential artifacts. Leave-one-out analysis highlighted a necessity of microphone placement behind the shooter and other less important microphones. Use of symmetry across the firing direction provides excellent results, generally below the 1 dB standard deviation. In the end, a best-practices guideline is given, which reduces number of required microphones by half. Through these analyses, future measurements will be more effective in microphone placement. With these level maps, one will also be able to better determine potential hearing risks associated with small firearm use and even avoid them through better drill.

Keywords: acoustics, rifle, gunshot, noise, interpolation, modelling, leave-one-out, symmetry, error, ghost points

ACKNOWLEDGMENTS

There are a more people I want to thank than I really can in this small section, but I will do my best. First, thank you to my parents for helping me follow my dream of a university education and also a Master's degree. You always pushed me to be my best, and I really appreciate it. Thank you to Dr. Anderson and Dr. Leishman for not only being on my committee, but also teaching me in several classes. Your love for acoustics shows, and it is infectious. Thank you, Dr. Gee, for everything. You have given me a lot of fun and unique projects to work on, and helped me improve myself more than just educationally. I know I was not always the perfect student, but thank you for always pushing me to do and be better. Lastly, thank you to all my fellow students and teachers, I would not be here without you all either.

Table of Contents

LIST OF FIGURES

Chapter 1

Introduction

In 2017, a large-scale measurement of the M16A4 rifle was made at Marine Base Quantico[1]. Small firearms have been measured before but not to the extent that was made over the course of this endeavor. Most efforts focused on simple analyses such as levels or limited directivity. The acoustic data recorded at Quantico will be used in an effort to better understand small firearm noise, as firearms reach potentially dangerous levels for human hearing, with 12.6% of Marines exiting basic training with hearing damage[2]. In 2009 alone, over $1.2 billion was spent on healthcare costs for 1.8 million veterans suffering from duty-related hearing damage[3]. This thesis attempts to combine interpolation and extrapolation, to predict range levels. Marines or recreational users can be regularly exposed, so qualifying the sound levels on the firing range will help to potentially limit harmful effects. By calculating associated errors and limitations, this thesis will serve as guideline for future measurements, and as a list of methods one can use to verify future datasets.

1.1 Small Firearms and Hearing Damage

On the gun range high intensity noise is present. The American Speech-Language Hearing Association (ASHA)[4] reports that levels can reach 140 dB to 170 dB depending on the weapon. Rifles fall somewhere in the middle, reaching levels around 160 dB depending on the firearm and the ammunition used. ASHA also reports that, “Exposure to noise greater than 140 dB can permanently damage hearing.” [4] The recommendations made by ASHA must however be taken with a caveat, as impulse noise often falls into a realm of unpredictability.

Early researchers attempted to understand impulse noise on hearing loss, but were less equipped to do so in the far field due to limitations in microphone density[5]. A-weighting can be applied to a waveform in order to mimic human hearing limitations. The National Institute for Occupational Safety and Health (NIOSH)[6] and the Department of Defense Instruction (DoDI 6055.12)[7] specify that sufficient hearing protection is required to keep personal noise exposures below an 8-hour time-weighted average (TWA) of 85 dBA (A-weighted) or 140 dB peak level. Murphy's group[8] did interpolation type calculations to determine that a 15 m foul line behind the shooter was roughly sufficient in most scenarios. Davis *et al.*[9] goes into more details about different criteria in relation to the Quantico measurement's in-ear reading.

Marshall *et al*.[2] sought to understand hearing loss caused from small firearms and followed a group of Marines through basic training. According to the study, during situations such as reserves and training schedules an average marine in training camp fires hundred or more rounds per week. Because a marine is not alone on the range, he or she also experiences the noise from his or her battalion's rifles. Unfortunately, they reported that 12.6% of marines exit basic training with some form of permanent hearing damage after only 10 weeks. While these measurements highlight the potential risks of small firearms measurements, further characterizations about the noise in general can be made.

1.2 Small Firearms Noise Background

Implementing proper measurement techniques and validations from the Quantico dataset, and any future datasets, will also allow for a better understanding of firearm noise propagation as a whole. This will in turn allow for safer drill or range design. In conjunction with these goals, results can improve MIL-STD-1474E[10] and ANSI/ASA S12.7[11], the standards for acoustic measurements of many military and impulse noise sources, which gives guidelines for measuring

small firearms including rifles, shotguns, and handguns. MIL-STD-1474E goes into instrumentation and recording, such as minimum signal-to-noise ratios and microphone requirements. It also defines relevant measurement conditions for recording, such as high-velocity winds, humidity, or excessive reflective surfaces. ANSI/ASA S12.7 focuses more on setup, such as angular resolution requirements for arc type measurements, or required sampling frequencies for accurate measurement. This standard approaches the acoustic or physics-based side of impulse noise measurements.

While small firearms have a long measurement history, most relied on minimal sampling locations. Their analyses focused mainly on weapons levels near the shooter[12], and were limited in scope. Weissler's[13] group noted multiple firearms exceeded the OSHA standard of 140 dB from a single shot. Rasmussen and Flamme[14] made significant contributions to measurement procedures, highlighting the importance of equipment with large bandwidth and high sampling rates. They also highlight some of the waveform shapes. Beck[15] and Routh[16] both focused on waveform characteristics along a radial arc, and may be the most extensive, noting events such as the ballistic shock, muzzle blast, and ground reflections.

One study performed by Routh and Mayer[16] focused greatly on the directivity of several small firearms. In their article they showed waveform recordings from locations along a polar arc spaced 16° apart to the right of the line of fire to directly behind the shooter. As the angle increased for a pistol, the pressure levels continued to drop. In the forward-facing direction, or line of fire, levels reached 8000 Pa, or 172 dB. In the rear, levels had fallen to 500 Pa, or 147 dB. While a pistol is different than the M16A4 Rifle of Quantico's data set, the data still serve as something to refer back to as a visual confirmation of data fidelity.

While Routh and Mayer made measurements of directivity, there is still a question of propagation out from the source. Murphy *et al.*[8] attempted to expand on this measurement and do multiple polar microphone arrays to capture how the noise propagated beyond 3 meters. They mainly focused on 8-hour A-weighted equivalent levels in attempt to find what they call the 85 dBA foul-line. This line, or more specifically going inside of it, typically represents where a human could suffer hearing damage. In their article they reported the interpolation for a single shot. This, and most of their interpolations presented, were given as 8-hour A-weighted equivalent levels[8]. This metric allows for easy conversion to noise exposure. For a single shot levels reached up to 56 dBA. Levels decayed radially from the source, with the fastest decay seen directly behind the shooter. Seeing similar trends in the data we analyze will help validate our recordings.

1.3 Objectives and Scope

The main purpose of this thesis is to create more accurate decibel level maps for both peak levels (L_{pk}) and 8-hour A-weighted equivalent levels (L_{Aeq8hr}). The maps range from 12 m behind the shooter to 6 m in front and from plus-or-minus 50 m to the left and right. This represents the likely area in which either marines or instructors would stand. The creation of these maps will rely on interpolation and extrapolation to understand these levels in locations on the range. As part of the work, a level maps calculator was developed for use. This calculator allows creation of different interpolations based on inputs such as, but not limited to, number of shooters, their spacing, and how many shots fired. These level maps do not come without potential errors. In order to understand the errors inherent to the data, the thesis will first focus on data validation. Typically, an error of 3-dB is associated with an operational doubling (or

halving) of shots allowed[17]. While some validation has been performed by Rasband *et al.*[1], this thesis will focus on defining an error limitation in terms of a decibel level.

After an error limit has been established, various analyses will be done to determine the importance of microphone placement and to find the most relevant locations for acoustic data recording. The efforts presented here will focus mainly on the standing, right-handed shooter configuration recorded at standing heigh microphones. Both the peak level and 8-hour A-weighted equivalent levels will be discussed. The first set of analyses will look at directivity and radial decay patterns. These will be useful for extrapolation. Then, by looking at each individual microphone's location as well as groups of microphones like microphones the left or right of the shooter, the most important locations can be determined in reference to these error limits.

This is not an all-encompassing foray into interpolation and extrapolation as a method for creating plots, but the techniques within this thesis can form a basis for plotting any future impulse measurements. For small firearms, and in particular the M16A4 rifle, predictive models will help to limit hearing damage, as well as inform future drill designs. While more recommendations will be made in the future by others, this thesis will help to further establish the foundation or standards for acoustic measurement of small firearms.

Chapter 2

Measurements of the M16A4 Rifle at Marine Base Quantico

In July 2017, sound measurements were made of the M16A4 rifle and Marine Base Quantico in Virginia. Recordings were made at an unprecedented 113 different locations on the range. This chapter discusses the various configurations and microphones set up at the

measurement site, as well as some goals associated with their deployment. One of the main goals of the thesis is to understand how microphone placement affects level maps created using a combination of interpolation and extrapolation. This chapter provides the background on the available microphones, as well as the microphones prioritized in the analysis chapters.

2.1 Test Description

In order to maximize range coverage, 113 microphones were used in specific configurations (Figure 2-1) explained in this chapter to acquire data. The microphones ranged from -46.5 m to 46.5 m along the x-axis of the range. In the y-direction, microphones ranged from -20 m out to 3.67 m. An aerial view of the setup with relevant locations is shown in Figure 2-2. This highlights that the range was not perfectly flat, and may lead to some microphones located at larger distances from the source and not exactly at 1.56 m.

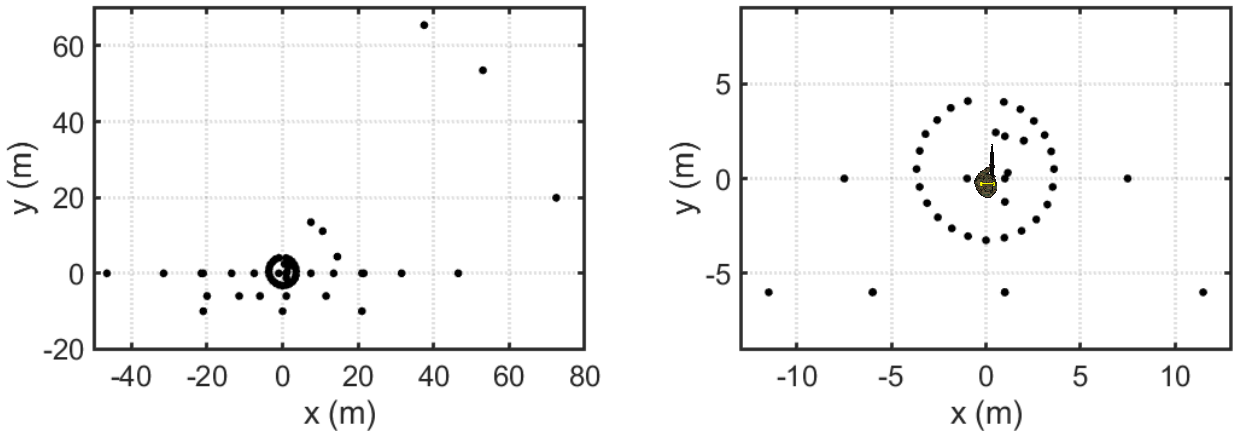

Figure 2-1 Schematic of microphone locations on the firing range. Shows various locations of microphones and stands. The right picture is a focused version of the left, showing rough shooter position.

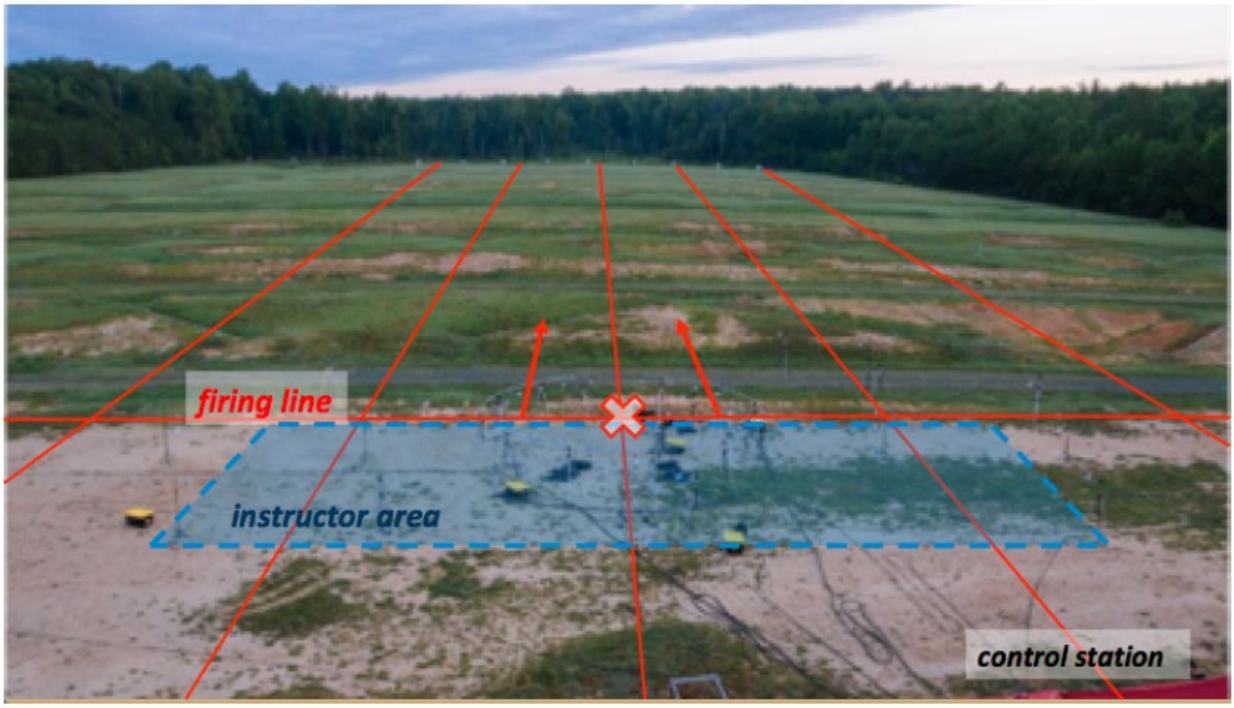

Figure 2-2. Another aerial view of the firing range, with locations labeled to clarify firing direction and general layout

A circular arc of radius 3.67 m (see Figure 2-3 left) surrounded the origin. Beyond those microphones, nine microphones were placed along three different radials (three microphones per radial not including arc microphone) in front of the shooter ranging out to 75 m.

Figure 2-3 Circular arc array with measurement team standing in the middle for scale.

To meet the guidelines set in MIL-STD-1474E[10] for assessment of levels at a listener's ear without a listener present (a "hearing zone" measurement), two roving microphone stands were employed to gather data at approximate head locations along the firing line (y = 0 m). Typically, they would be in positions where shooters would stand along the firing line, generally in increments of 3 m, and were moved in between recordings of different 10-round firings. Note that the weapon's muzzle location was always at approximately y = 0.5 m, in front of the lineup. These roving microphone stands allow for microphone placement in a location where a shooter would normally be. While the interaction between a microphone and a human ear may be different, it still provides a slightly more accurate recording.

Both the roving microphone stands and other microphone stands along the firing line employed microphones at three heights. These "3-height" microphone stands were used to mimic the heights of the shooter in the standing (1.56 m), kneeling (1.09 m) and prone (0.35 m) positions, as seen in Figure 2-4, emulating a previous study by Wakefield[18]. While slightly different from the standard, the heights were selected to better represent the M16A4 Rifle. The microphones at standing height (1.56 m) were pressure microphones oriented skyward, while the other microphones were the free-field type and pointed towards the source.

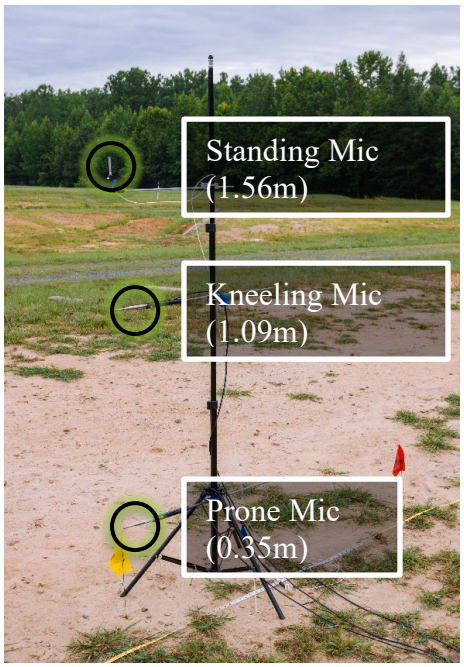

Figure 2-4. Multiple-height microphone stand in the field. Microphone heights are labeled.

To ensure quality data acquisition, all microphones were calibrated in-house using a GRAS 90CA-S2 calibration system. Microphones were assigned to measurement locations based on their sensitivity and according to an estimate of levels compared to a model of spherical spreading. For locations near the origin, microphones with the lowest sensitivities were chosen. Microphones were also field-calibrated using GRAS 42AB calibrators on the day before the test, right before the first measurement, and after the last measurement. Variations in sensitivity were generally less than 0.2 dB.

The arc microphones around the central location (see Figure 2-3) were spaced in 15° increments, with no microphone placed at the 0° angle (along the firing direction) allowing the shooter at the origin to more easily shoot downrange. Positive angles are represented as going clockwise from the firing direction. The microphones were mounted on a 4-m radius arc that was fabricated at BYU from pieces of 1” square aluminum and assembled in the field, such that the

microphones were located at an effective radius of 3.67 ± 0.02 m from the arc center, with the weapon muzzle located at the arc center. All microphones were the same height.

Lastly, seeking to understand where the sound was originating on the weapon, a 16-microphone pentaskelion (5 arm spiral) beamforming array, located 1.5m away, was pointed at the M16A4 Rifle. While this thesis does not focus on the beamforming analysis, it will allow for a future in-depth analysis of sound characteristics of the rifle itself.

2.2 Microphone Types

For the majority of the locations, ¼" microphones were utilized. These microphones were selected due to their low sensitivities, which allow for clean data acquisition. The ¼" microphones used were a combination of GRAS 46BE, 40BD, 46BG, and 46BD types. The 46BE microphones all used ½" preamplifiers and were utilized on the arc as well as at standing and kneeling heights. The other microphones were placed according to sensitivity and distance to source.

At locations extremely close to the source, e.g., 1 m away, PCB 137B21B intensity probes were utilized as shown in Figure 2-5. These probes, called "pencil" probes due to their design, are used for measuring blast sounds. These probes have a high noise floor, and were best used only in peak level calculations. Even so, the recorded waveforms were much noisier than a standard ¼" microphone. These pencil probes could not be calibrated, and relied on manufacturer specified sensitivities. At the range, pencil probes were "tap-tested"; by lightly tapping on the microphone, one could detect that a signal was measurable.

The last sets of probes were custom GRAS 3D Vector probes[19] also shown in Figure 2-5.The probes contain four phase-matched 40BH pressure microphones in a tetrahedral shape.

Because of its 3D design, the probe allows for full characterization of the intensity vector. These microphones will not be a source of analysis in this thesis, but may allow for future intensity analysis. These intensity probes, like the pencil probes, relied on manufacturer sensitivities.

Figure 2-5. (Left) PCB 137B21B Pencil probe. (Right) Image of GRAS 3D Vector Probe.

2.3 Shooter Configurations

Over 54 different shooter configurations were tested in order to maximize the analysis potential for the M16A4. Figure 2-6 highlights configurations example for a standing, kneeling, and prone shooter. Other variations in configuration include:

- Occupied range (consisting of one shooter in the center and 12 additional personnel not firing weapons spaced every 3 m to the left and right) vs. unoccupied range (single shooter only).
- Left-handed vs. right-handed shooter.
- Gun stand with a low acoustic profile to eliminate effects of scattering off the shooter's body.
- Marine position either at -18 m, 0 m, or 18 m along the firing line.

- Multiple shooters vs. single shooters.
- Variable locations of roving microphones along the firing line.
- Standing (1.56 m), kneeling (1.09 m), and prone (0.35 m) shooter position, as mentioned.

In each configuration, any shooter would fire up to 10 rounds of ammunition. At minimum, each recording contains at least eight impulse events, which depended on the communication between shooter and recording software operator. This is above the threshold of five impulses outlined in MIL-STD-1474E[Error! Reference source not found.].

Figure 2-6. Images showing a standing, kneeling, and prone shooter. The low acoustics profile mechanical shooter stand is shown on the far right.

By making recordings of all of these configurations, a rich dataset was generated with many more analyses available than what had previously been done. Each comparison can help in drill design or overall guidelines for firearms usage. The main focus of this thesis is standing

right-handed shooters, as mentioned in the introduction, but will show results as well for other comparative configurations.

Chapter 3

Data Validation

This chapter discusses some methods used to verify that the data collected at Quantico are valid for further analysis. The primary points of discussion are the waveforms and their levels. Along with that, several important metrics are discussed as relevant to the motivation for the research. Next, an error bound is defined for analyses shown in Chapter 4 and Chapter 5. Lastly there is a brief discussion on the polar measurement arc, and the spacing of sampling points. Looking at standard deviations between shots, it is reasonable to see up to 1 dB of difference for any metric at a single microphone location over a 10-shot volley of a configuration type.

3.1 Waveforms and Levels

While more microphones were deployed, the ones shown in Figure 3-1 are the ones used for the primary analyses shown for verification and level maps. These microphones are all at the standing shooter height (1.56 m), and were chosen due to level map relevance. For a standard firing range exercise, shooters and instructors would either be on or behind the firing line. For that reason, it is practical to focus on this section of the range. While further analyses could be done on the kneeling and prone height microphones along the firing line, the level-maps section will focus mainly on the standing height. By solidifying the analysis approach, further inquiries into microphone height can be made beyond the minimal analyses shown in this thesis.

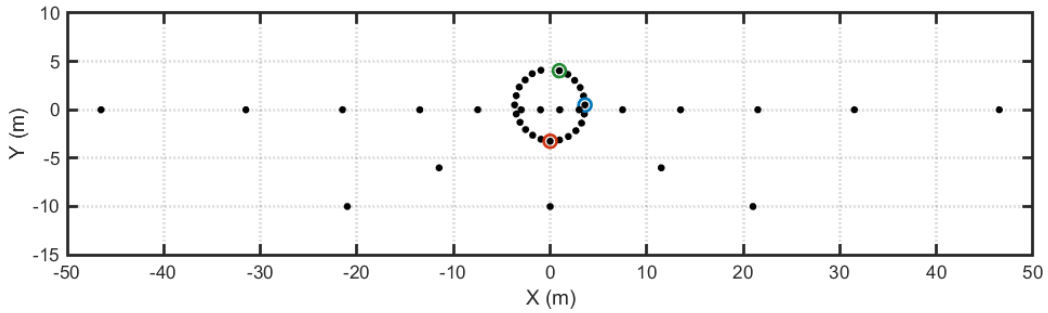

Figure 3-1. Microphone locations used for analysis. Three microphones on the polar arc array are highlighted for reference in Figure 3-2.

Figure 3-2 highlights three different pressure waveforms measured at locations on the arc as shown in Figure 3-1. Positive angles are measured clockwise from the firing direction. The recording at 15° notably contains both the ballistic shock and muzzle blast, while the other two waveforms do not. The recording at 180° is not only quieter, but the ground reflection is not as readily identifiable. Both measurements at 15° and 90° have clear ground reflections. These waveforms show the angular differences along the arc. As one would assume, the source is not perfectly symmetric.

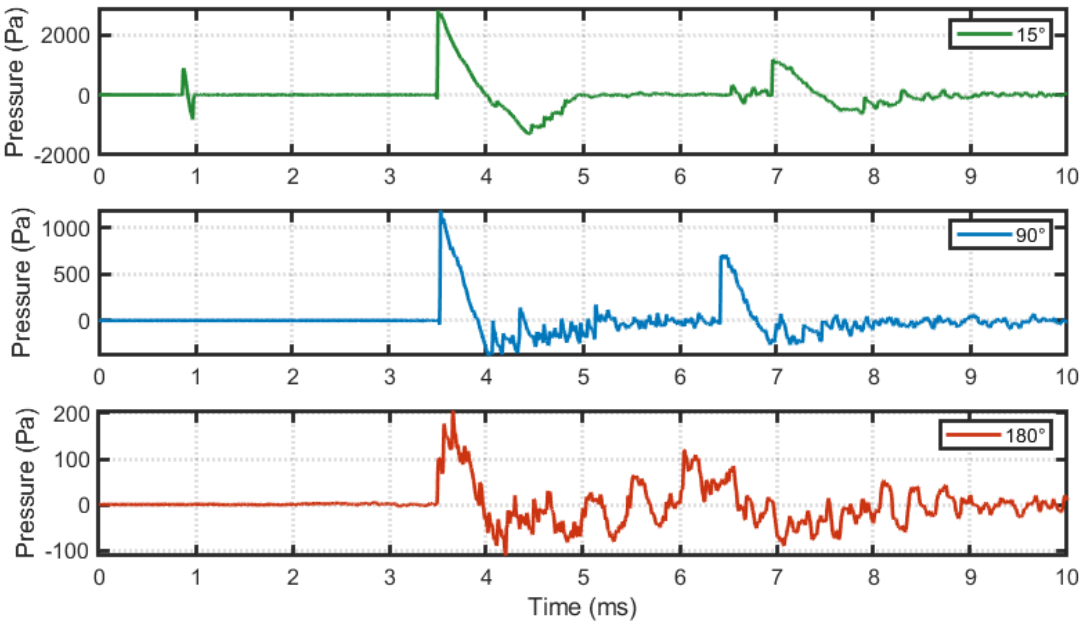

Figure 3-2. Time waveforms from three microphone locations along the polar arc. These locations are highlighted in Figure 3-1. Positive angles are measured clockwise from the firing direction.

Comparing back to Routh's arc-type measurement results of the AR15 rifle[16], one sees a similar trend. The front of the shooter recorded the highest levels. Routh and Maher reported 8000 Pa in front then moving to 2000 Pa and finally 500 Pa at the side and behind respectively. Their arc was slightly closer than the Quantico set, and their shooter was sitting on a stand with firearm roughly 1 ft above the arc. Moving from the front to the back following the arc showed the effects of shielding, and that there was a ballistic shock in the forward-facing direction. Using pressure values given by Routh and Maher, peak levels can be plotted against the peak levels recorded at Quantico. These results are shown in Figure 3-3.

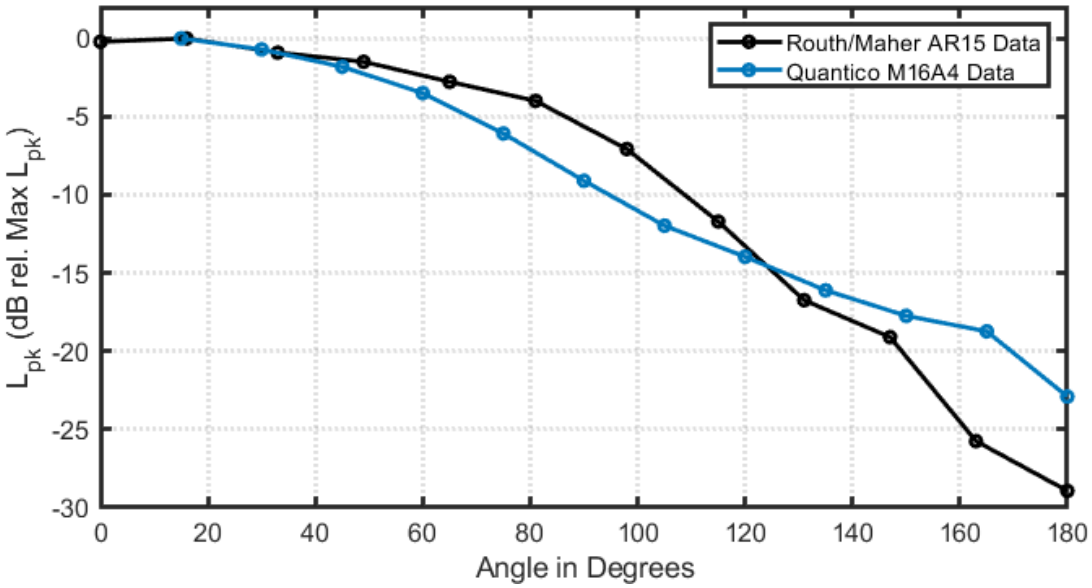

Figure 3-3. Directivity comparison of the AR15 rifle data measured by Routh and Maher[16] in 2016 and the M16A4 rifle data measured at Quantico Marine Base in 2017. Levels are plotted as the difference between the measured the peak level (L_{pk}).

Figure 3-3 uses Routh and Maher's[16] data to help validate the results seen at Quantico. Both weapons see a decay in level as the azimuthal angle increases. The AR15 data sees a steeper roll-off at large angles, or behind the shooter. This could be due to measurement geometry, and the recordings of the AR15 were made below the source. A shooter would potentially shield the rear more, leading to a faster level decay. That all said, the overall trend is consistent, with peak levels being highest at 15° from the firing direction, further validating the Quantico data.

3.2 Metrics

The two main metrics this thesis focuses on are the peak level (L_{pk}) and the 8-hour A-weighted equivalent level (L_{Aeq8hr}). The peak level gives a better physical representation than an energy-based metric. By taking the highest measured pressure at each location, comparisons can be made in a one-to-one manner with other configurations or measurements.

The L_{Aeq8hr} allows for easy comparisons to dosages or exposure limits. As Murphy *et al.*[8] has done, one could potentially calculate an 85 dBA foul line, or location inside which hearing damage is possible. There are multiple models for noise exposure from small firearms, but sticking with a well-known A-weighted equivalent level reaches a broader audience. Should anyone care purely about the energy that each shot produced, for most close microphones, a 10-millisecond equivalent level (L_{eq10ms})[1] or sound exposure level (SEL), could also be used, as it encompasses all components of a shot event. However, peak level is typically a consistent measurement of shot level. This thesis will only focus on the two metrics, but an SEL or L_{eq10ms} could be useful in the future.

3.3 Shot-to-shot Consistency

In each configuration, between 8-10 shots were fired in succession. Figure 3-4 shows 9 shots aligned on the muzzle blast recorded from a standing right-handed shooter on an unoccupied range. Shots were recorded on the arc at the 15° location (green location in Figure 3-1). All nine shots are visually consistent with each of the four major energy components identifiable: ballistic shock, muzzle blast, and their respective ground reflections. While the muzzle blasts are time-aligned, the ballistic shocks are clearly not. This is due to the angle at which the shooter was firing. While shooters were firing at targets far downrange, even the slightest angle change can alter arrival times of the ballistic shock. Due to the clustered nature of the waveforms, one can infer that the shooter started firing a little more in the positive angular direction after shot 6.

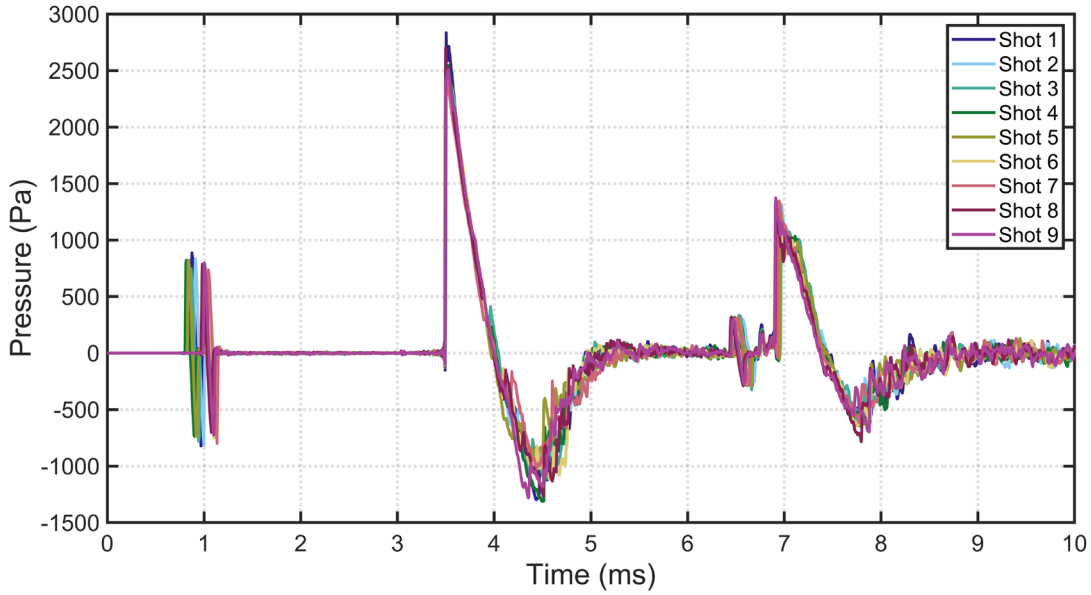

Figure 3-4. Time waveforms recorded along the arc at 15° (clockwise from the firing direction) aligned on the muzzle blast rise. For this configuration, nine shots were recorded.

Taking the standard deviation of peak level (L_{pk}) for these 9 shots results in a deviation of 0.81 dB. This might be due to slight differences in shot angle, slight shooter location adjustments, or even the amount of gun powder within the bullet. Repeating this standard deviation calculation at each measurement location results in 46 different values, which can then be plotted on a histogram as seen in Figure 3-5, to see overall deviation patterns across the range.

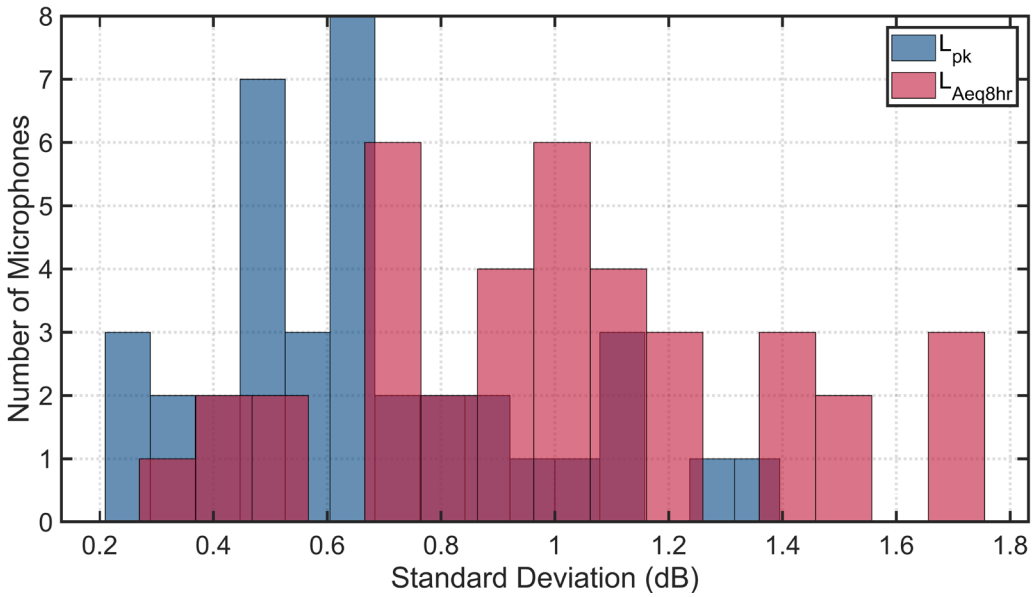

Figure 3-5. Histogram of different microphones standard deviations of peak and 8-hr A-weighted equivalent levels for a standing right-handed shooter. Standard deviations were calculated for each microphone location using levels from each of the nine shots recorded.

The vast majority of deviations, particularly for peak levels, falls below 1 dB, with the mean for the level equaling 0.7 dB. For the 8-hr A-weighted equivalent level (L_{Aeq8hr}), standard deviations are slightly higher with a mean of 1.0 dB. These deviations will serve as a baseline in determining error significance. If an interpolation or post-processing effort leads to less than 1 dB of change, it is assumed to be within the realm of shot-to-shot deviation, and acceptable as a means for prediction judged be practical. Any error beyond 1 dB must be accounted for and effects must be evaluated on a per-measurement-analysis basis.

3.4 Polar Arc Limitations

Sparse microphone resolution can lead to poor interpolation values. The ANSI S12.7 standard[11] calls for a 30° polar arc resolution, but even this may not be fine enough. By removing one microphone along the arc and interpolating using the two adjacent microphones, a comparison can be made for the right-handed shooter instance. The differences are shown in

Table 3-1. The L_{pk} has significant differences in levels when interpolated. This is most apparent in the rear at ±180°, where differences are 2.1 dB for the L_{pk}. For right or left-handed shooters, the effects are consistent; there is a more significant error in the rear. The recorded levels for the shooter stand saw less variation in the rear, only reaching 1 dB. However, the shooter stand is less valuable in simulating real environments or computing real exposures for firearms measurements.

TABLE 3-1. Difference between recorded peak levels and peak levels acquired through interpolation from the nearest two microphones along the microphone arc. An extended table with equivalent levels in shown in the appendix.

Angle	-75°	-60°	-45°	-30°	-15°	0°	15°	30°	45°	60°	75°	90°
L_{pk} Error (dB)	0.6	-0.1	0.3	0.3	0.4	-	0.4	0.2	0.3	0.5	0.2	-0.1
Angle	105°	120°	135°	150°	165°	±180°	-165°	-150°	-135°	-120°	-105°	-90°
Lpk Error (dB)	-0.4	0.1	-0.3	-0.3	1.6	-2.1	-1.8	0.6	-0.2	0.4	-0.5	0

As mentioned above, the ANSI S12.7**Error! Reference source not found.** standard calls for 30° resolution for arc-type measurements. This is adequate to the sides of the shooter; however, 15° resolution is more ideal in the rear and potentially near the edge of the ballistic shock cone. Without a 15° resolution, errors can reach up to 2 dB, greater than the shot-to-shot deviation. At these locations, interpolation can cause larger errors, which will be highlighted in Chapter 5. However, before interpolation results can be discussed, the thesis will first need to discuss differences between shooter comparisons.

Chapter 4

Shooter Type Comparisons

This short chapter will discuss the effects of some shooter configurations. At Quantico, measurements were made with standing, kneeling, and prone marines. For each of these three configurations measurements were also made of a left-handed, and a right-handed shooter, as well as a mechanical shooter stand. The goal of this section is not to analyze the effects of the configurations in depth, rather to show some of similarities and differences. This allows for comparisons between further analyses and determine if similarities or differences persist on a broader scale.

4.1 Shooter-handedness

The bulk of the modeling discussion will focus the right-handed standing shooter on an unoccupied range, however, polar plots shown in Figure 4-1 highlight differences and similarities between the 'three' shooter handedness. For both L_{pk} and L_{Aeq8hr}, the right- and left-handed shooters see similar results. For the peak levels, the only differences are behind the shooter, and it falls within the 1 dB shot-to-shot deviation. The shooter stand, as shown in Figure 2-6 on the far right, has less shielding in the rear, but is similar in directivity shape to the left- and right-handed shooters. The left-handed shooter is overall slightly quieter than the right-handed shooter in terms of the equivalent level. For both metrics, the shooter stand configuration produces a slightly higher level on the left side of the shooter, perhaps denoting some cushioning provided by the marine. It should be noted that the guns are the exact same for both left- and right-handed shooters. There are no modifications made for a leftie.

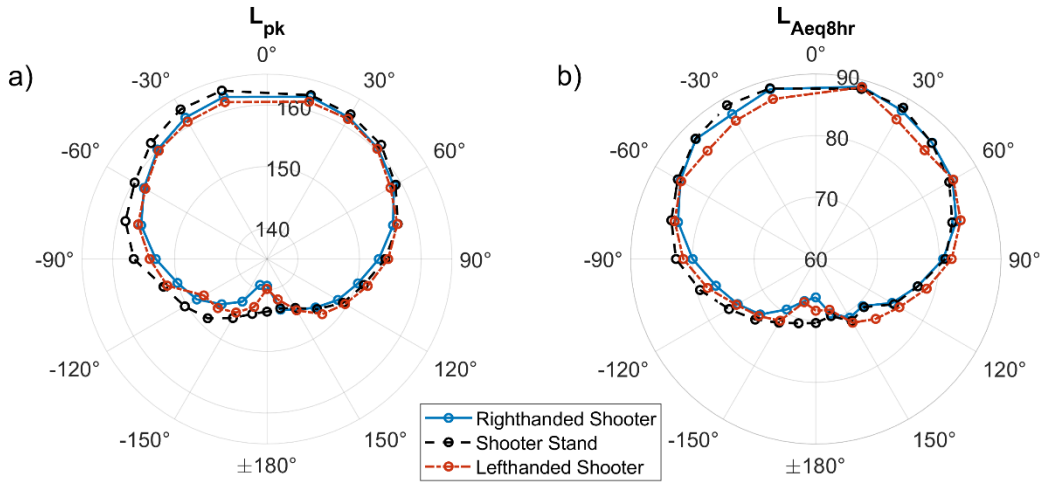

Figure 4-1. Polar plots of both peak and 8-hr A-weighted equivalent levels for both right-handed and left-handed shooters as well for the mechanical shooter stand at standing height.

For future measurements, it is relevant to do all three shooter types where possible. For most weapons, there are not different left-handed and right-handed weapon variants, nevertheless a change in shooter-handedness can be significant. There could be interplay between the shooter's stance providing baffling and the firearm (for example, a right-handed shooter has the butt of the rifle in his right shoulder, while it is opposite for a left-handed shooter). In the forward-facing direction, peak levels are consistent between right- and left-handed shooters, with an average difference of 0.95 dB. In the rear, differences could reach up to 2.5 dB. This reinforces the idea of careful measurement of locations behind the shooter. The equivalent level sees larger differences in front of the shooter, with some differences reaching 2.68 dB. A shooter stand is helpful, but less relevant for exposure type calculations, as it is uncharacteristic of a drill or range environment. For exposure-oriented research in particular, each measurement should repeat configurations with both a left- and right-handed shooter where possible.

Unfortunately, by changing shooters per configuration, there was some deviation within source location. By using three microphones of known locations, localization analysis can be done using relative arrival times of muzzle blasts and assumed speed of sound. This analysis showed a range of roughly 1 ft from the planned source location. Using an assumption of spherical spreading to help see the potential peak level change along arc measurement locations, this 1 ft range can mean up to 1 dB of difference. This adds further uncertainty within comparative tests across different configurations. A shooter stand can provide consistency compared to a human counterpart, and could be used to better compare measurements of the same firearm, but in a different setting.

4.2 Standing, Kneeling, and Prone

In order to determine the importance of measuring each shooter configuration, comparisons were made of waveforms generated from all combinations for standing, kneeling, and prone microphone and shooter heights. This thesis chose to look at the three-microphone stand 7.5 meters to the left and right of shooter. Although there are more options to choose from, this is limited the analyses to these locations, and looking both at the left- and right-handed shooter cases shown in Figures Figure 4-2 through Figure 4-5. As the three configurations are done with different measurements, and with potential shooter changes between them, the levels will differ slightly between the measurements. Each row in a figure represents one measurement configuration, but are plotted together for comparison. Trends and overall shapes are considered more than levels.

The first case shown in Figure 4-2 is for a right-handed shooter at the microphone stand 7.5 m to the right of the shooter along the firing line. One of the big questions to answer is the idea of reciprocity. Does a prone shooter generate a similar waveform at the standing height

microphone as a standing shooter would generate at a prone height microphone? For this first case, and consistent throughout the others, it does not. This means that one cannot cut corners and only change shooter heights or microphone heights. In order to be comprehensive, one needs to do these nine configurations for every test.

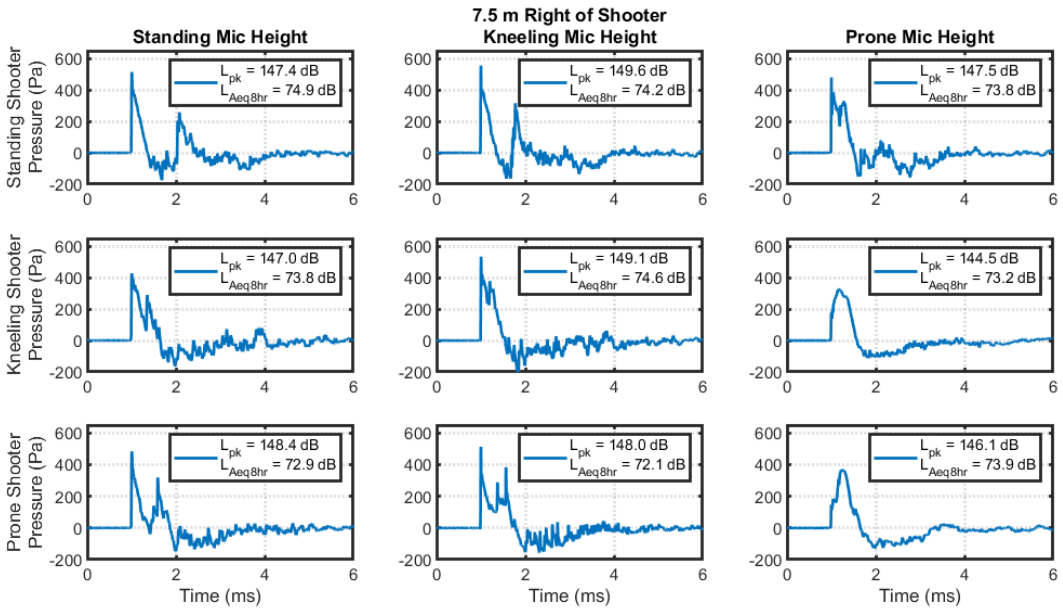

Figure 4-2. Time waveforms for standing, kneeling, and prone **right-handed** shooter and microphone combinations 7.5 m **to the right** of the shooter. Legends show average peak or 8-hour A-weighted equivalent levels for all shots of this configuration at the locations specified.

As the microphone gets closer to the ground, there is a merging of the incident and reflected waves, and as the shooter approaches the ground, there is less of a sharp peak in the muzzle blast. This is only consistent to the right of the shooter, but does not change between the left- and right-handed shooter. This could be an effect of the source, but unfortunately, there is no data to compare back to at the prone height. The two recorded metrics, peak level (Lpk) and 8-hour A-weighted equivalent level, do not show significant differences as an overall trend. Again, the level spread is only 3 dB again. This is consistent for both left- and right-handed

shooters, as well as to the left and right side of the shooter. This could prove impactful in a potential future analysis.

For the microphones situated 7.5 m to the left of the shooter, as shown in Figure 4-3, one sees similar trends with incident and reflected ground waves merging. The prone height microphone does not lose the sharpness in the peak like the microphones to the right of the shooter, however. There is no trend between standing, kneeling, and prone microphones and shooters. There is roughly a 3 dB spread between the highest and lowest recorded levels.

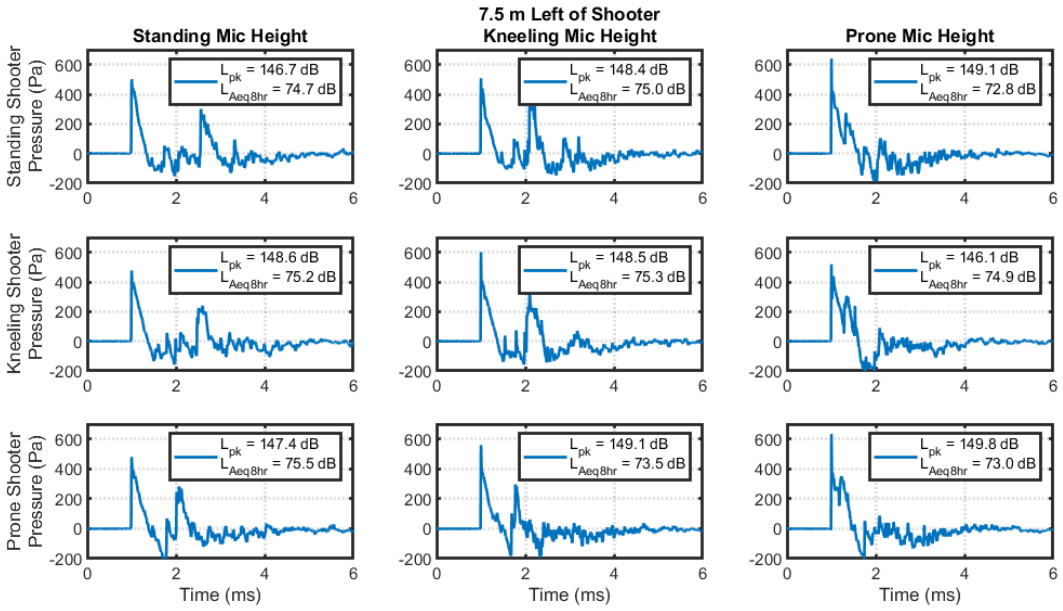

Figure 4-3. Time waveforms for standing, kneeling, and prone **right-handed** shooter and microphone combinations 7.5 m **to the left** of the shooter. Legends show average peak or 8-hour A-weighted equivalent levels for all shots of this configuration at the locations specified.

Figures Figure 4-4 and Figure 4-5 show results for the left-handed shooter. Again, as the shooter and microphone combinations get closer to the ground, the tighter the incident and reflected pressures become. The prone height microphones to the right of the shooter are more rounded, just like in the right-handed shooter, meaning it is not reliant on shooter-handedness.

Overall, it is difficult to see much of a difference between a left- and right-handed shooter from these waveforms alone.

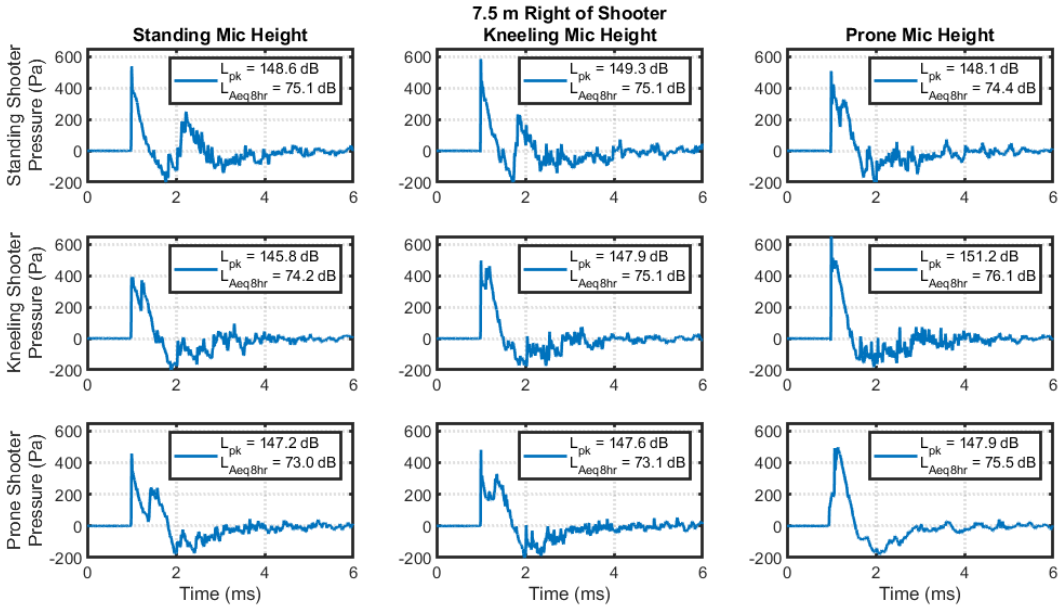

Figure 4-4. Time waveforms for standing, kneeling, and prone **left-handed** shooter and microphone combinations 7.5 m **to the right** of the shooter. Legends show average peak or 8-hour A-weighted equivalent levels for all shots of this configuration at the locations specified.

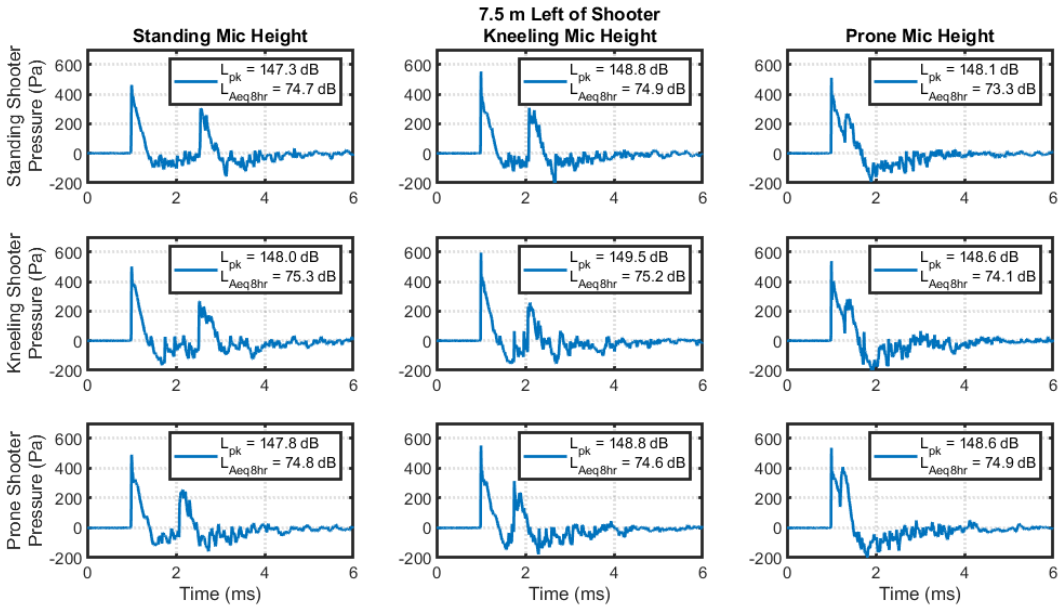

Figure 4-5. Time waveforms for standing, kneeling, and prone **left-handed** shooter and microphone combinations 7.5 m **to the left** of the shooter. Legends show average peak or 8-hour A-weighted equivalent levels for all shots of this configuration at the locations specified.

The biggest takeaway from this waveform analysis is that it is important to have all of the microphone and shooter height combinations measured that would correspond to any real scenarios. There is roughly a 3 dB spread between all types of combinations, and the patterns are inconsistent. Were someone only have time for one configuration, he or she could add a blanket 3 dB to the prediction made. This would be a conservative estimate, but is a better approach for limiting dosage than nothing. For the military, they do drills in standing, kneeling, and prone postures, and it makes sense to record all of these in order to better predict potential hearing risks associated with the firearms. In a recreational range, it might make more sense from an efficiency standpoint, to only do microphones at the standing heights, and focus on covering more ground in the x-y plane.

Chapter 5

Level Maps

This chapter will show effects of different types of interpolation approaches on generating level maps for the M16A4 rifle. The primary focus will be on the standing right-handed shooter configuration; however, additional plots for different shooter configurations are shown in the appendix. The first point of discussion is on radial decay, which sets up the idea of ghost points, as well as decay rates as a potential means of map generation. Using either Cartesian or polar interpolation leads to different effects, but it is shown that Cartesian interpolation with use of ghost points is a more reasonable prediction of the levels in the field. Using this Cartesian interpolation, one can then compare other effective data sets against it as a baseline. By doing so, one can recommend microphone locations as well as determine the most important sampling points for small firearms measurements.

5.1 Radial Decay

In order to help better understand the sound propagation of the M16A4 rifle, peak levels were plotted along radials from the source. Unfortunately, not all radials had the same sampling points, but regardless, are shown in Figure 5-1. Levels decay as distance from the source increases, as one might expect. There are three types of decay briefly considered here: basic spherical spreading, nonlinear decay, and a blast wave assumption, with decay slightly faster than spherical spreading.

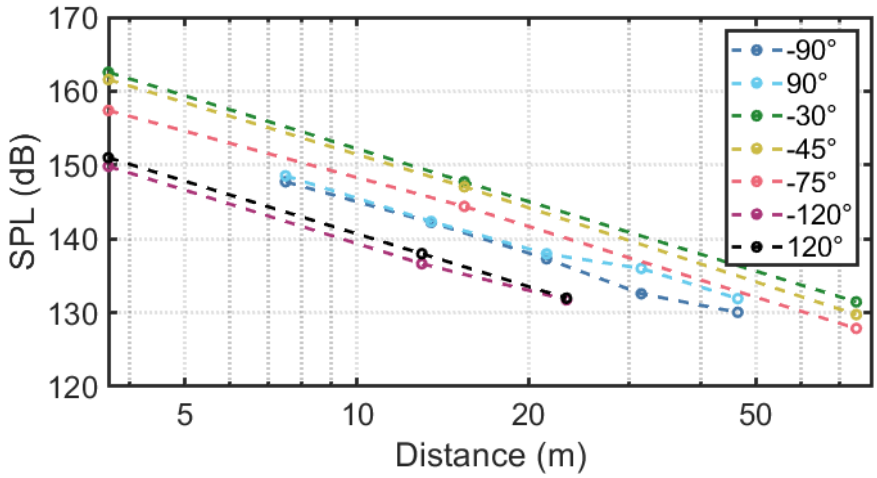

Figure 5-1. Peak levels for radials measured for a standing, right-handed shooter. The direction of fire is at 0° with positive angles measured counterclockwise.

One of the possible decay patterns for small firearms is a nonlinear spreading. Following a weak shock prediction[20,21], one can attempt to match the data points to a predicted roll-off for this simple shock equation. This type of prediction sees steep roll-off in the near-field while approaching a 24.0 dB per decade decay in the far-field. While a nonlinear decay rate is harder to justify, one can also check a spherical spreading decay rate, or 20 dB per decade.

According to ANSI S2.20–1983[22], there is a predicted roll-off of $r^{-1.1}$ for explosive-type sources. That means it is slightly faster than a spherical spreading or $r^{-1.0}$ roll-off. This corresponds roughly to a 22.0 dB per decade roll-off in terms of level against distance, versus spherical spreading's 20 dB per decade. There is an argument that a gunshot is a more condensed small explosion, and this type of decay could be a good measurement ideal, but this thesis will not focus on proving this decay pattern. The important point made here is that one can use spherical spreading as a conservative estimate for level decay. By overpredicting levels, marines

or recreational users can be overprotected. When it comes to protecting from hearing damage, a conservative approach can be beneficial.

5.2 Interpolation

There are two main types of interpolation to choose from: Cartesian or polar. Cartesian interpolation relies on bicubic interpolation along the x-y coordinate system, while a polar interpolation relies on the thin-plate interpolation in the r-θ coordinate system. For this thesis, Cartesian interpolation will use the regularizedata3D function found on MathWorks[23], while the polar interpolation will use the MATLAB built-in function 'fit.' Plotting both for the standing right-handed shooter gives insight into their merits.

The first approach taken is using polar interpolation using a thin-plate fit. Using a thin-plate fit helps with a non-uniform grid in the x-y plane, or as one might expect from a polar-oriented grid. One might think this would represent the source well, especially with the polar arc three meters away, but this approach has some flaws. Figure 5-2 highlights some potential issues using this method.

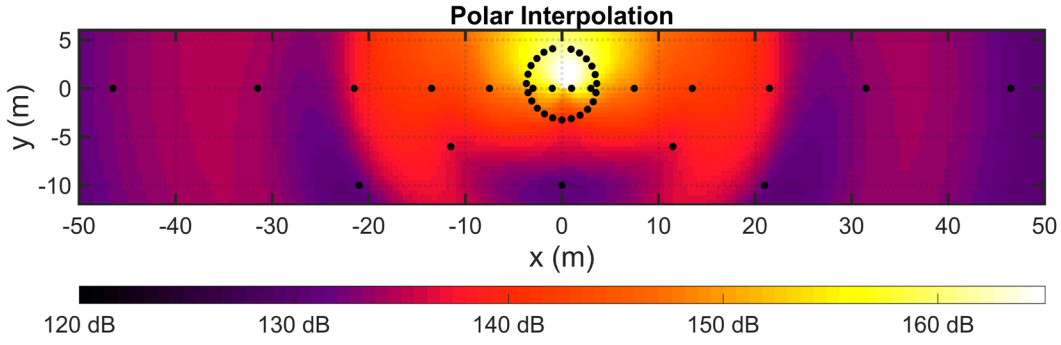

Figure 5-2. Peak level map for a standing, right-handed shooter created using a polar interpolation scheme. Black dots represent microphone locations.

The polar interpolation shown in Figure 5-4 highlights some source effects, isolating the source in the middle of the polar arc array. Unfortunately, there seems to be some sort of oscillatory behavior as the sound propagates away from the source. This is seen along the firing line, as the levels go down around x = 28 m, but then go back up by x = 35 m before finally decaying. These artifacts persist for any metric used, and are not what one would expect. Nevertheless, the polar interpolation does do well in predicting levels at the extremities. The interpolation sees rapid decay at the edges of the interpolation range rather than approaching a constant or linear decay, but the overall decay pattern makes sense. The next option for interpolation is using a Cartesian interpolation map. Using the function regularizedata3D[23], one can generate Cartesian interpolations with ease and can also adjust precision. The interpolation method used here is bicubic. This a good approach for a Cartesian mesh with equal spacing. Even with minimal smoothing, one can generate the plot shown in Figure 5-3.

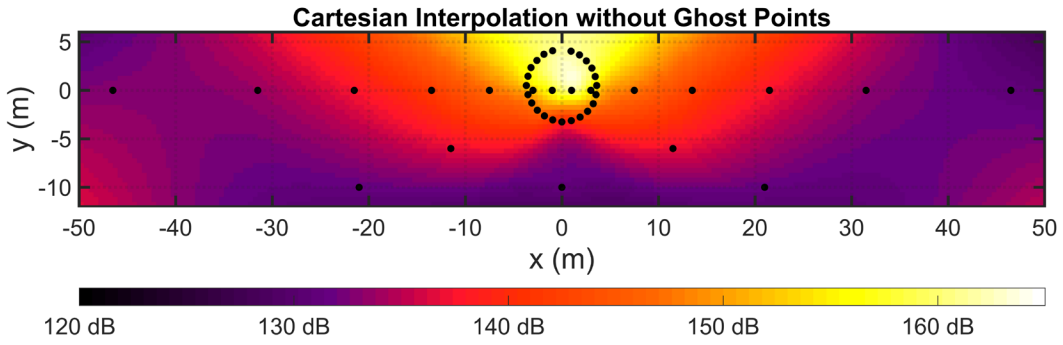

Figure 5-3. Peak level map for a standing, right-handed shooter created using a Cartesian interpolation scheme. This relies on the function 'regularizedata3D' found on Mathworks[23]. There are no ghost points in the corners for this plot. Black dots represent microphone locations.

The Cartesian interpolation style also performs to an extent, but still runs into some problems at the extremities of our plotting range. There seems to be a tendency in front of the shooter to have levels begin to creep up. Again, not a perfect interpolation approach. The decay rate seems

to be more physical and there is less oscillatory behavior. While the Cartesian interpolation performed better overall, polar type interpolation could still be beneficial in creating a baseline plot. For this reason, ghost points were considered.

5.3 Ghost Points

For the purposes of this thesis, ghost points are defined as coerced level values at specific points within the interpolation range. One noticeable issue with the Cartesian interpolation was at or near the map corners. By using a prediction based on spherical-spreading, conservative estimates at the corners could be made. One could then set these estimated levels at the extremities of the map as ghost points for interpolation. The interpolation would then benefit from a radial interpolation to the corners, while maintaining the overall shape of the Cartesian interpolation.

Using spherical spreading as a guideline, ghost points can be placed at the corners of the map to smooth interpolation artifacts. As discussed in section 5.1, this is a conservative estimate, but will help smooth some of the interpolation artifacts. Ghost points are calculated by creating a line from the corner to the origin, finding the nearest point to the line, and extrapolating out from that data point to the corner. This creates a conservative estimate at these locations. The points farthest from the source tended to increase in level, which makes no physical sense, but by using ghost points, this issue can be avoided. The results for the peak level of a standing, right-handed shooter is shown in Figure 5-4. The combination of Cartesian interpolation and ghost points gave a much more physical solution, as levels decayed as distance from the source increased. Polar interpolation can use ghost points, but they are more difficult to argue for. If one were to use ghost points to smooth polar-interpolation artifacts, they would be placed behind the shooter.

While it is possible, the ghost points would have a larger influence on predictions between data points.

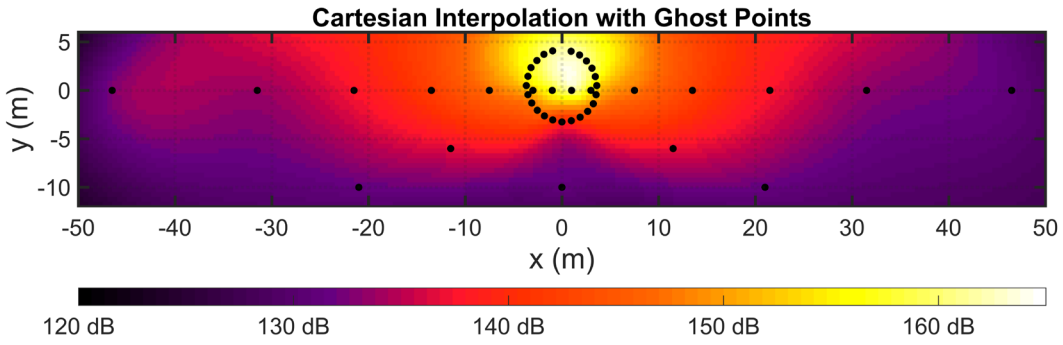

Figure 5-4. Peak level map for a standing, right-handed shooter created using a Cartesian interpolation scheme. This relies on the function 'regularizedata3D' found on Mathworks[23]. Ghost points were implemented at each of the corners as well as in front of the shooter. Black dots represent microphone locations.

Because ghost points are used at the corners of the plotting range, one might think to add ghost points at many locations. With the Quantico measurement, the source location (shooter) was changed to either 18 m to the left or right of the origin. By changing source locations while retaining microphone positions, total effective sampling locations were increased. While one could use these data points to artificially add data points to a data set, this is not the purpose of this chapter or thesis. Alan Wall *et al.*[17] did an analysis of the Quantico data with these ideas in mind, comparing a multi-shooter configuration to artificially placing shooters at locations along the firing line. They concluded that the error fell within an acceptable range of 3 dB.

If one wanted to maximize their microphone placement efficiency, he or she could record the shooter at locations all around the range to artificially extend spatial resolution. Rasband *et al.*[1] roughly demonstrates this, comparing recording locations along the firing line as measured

from different source origin. The multi-origin approach does lead to difficulty using free-field microphones, as they would not always face the source. For the purposes of this thesis, however, the author assumes that only one source location will be recorded.

5.3 Baseline

As shown, there are multiple approaches available for developing interpolated level maps, each with its pros and cons. In order to have a baseline metric with which to compare all future analyses to, a single interpolation approach was selected. A Cartesian-based interpolation with four ghost-points in map corners was selected, as this represented a conservative physical response for the source. Levels at the edges were a slight overprediction. Using results from Section 5.1, this is most likely 3 dB higher than what should be measured. While this is not ideal, it is better to overpredict at the limits than to underpredict.

The dataset contains many possible options for comparison, but this thesis will mainly focus on the peak level for a right-handed shooter in an unoccupied range at a standing height for the remainder of the discussion. Some further maps will be shown in the Appendix B. Both left-handed and shooter stand variants showed similar results and any approaches for error-analysis of the before-mentioned configurations are mostly applicable. This is also true for each level metric, whether peak or A-weighted equivalent level. The baseline interpolation map produced for the configuration is shown in Figure 5-5.

The baseline interpolation map highlights some effects of the firearm. As the sound travels out from the source, decay is present, although not perfectly spherical. The map is at first-glance symmetric about the y-axis, but not a perfect mirror. Lastly, shielding from the shooter rear is highlighted in the negative y-direction. Using the available microphone locations marked as black dots also gives guidance on future measurements, as locations of minimal data points

are apparent. All of these effects will be discussed in the scope of dB-differences from this baseline map.

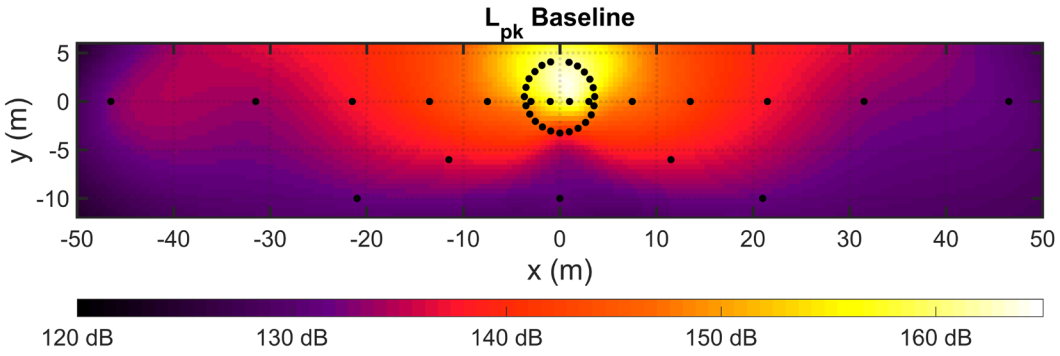

Figure 5-5. Baseline interpolation model of the peak level using all data points, Cartesian interpolation, and ghost points in map corners. All future comparison plots will be related back to this interpolation. Black dots represent microphone locations. Level limits adjusted from Figure 5-5.

Using the baseline and the error analyses given in this section, one can determine more important microphone locations, and potentially where one does not have to be as thorough in placement. The best case will always be to collect as many data points as possible, but with limitations either due to equipment or time, best recommendations will be given. We will show analyses mostly on the peak levels, but the same ideas are applied to the 8-hr A-weighted equivalent level as well. The baseline for this equivalent level is seen below, in Figure 5-6

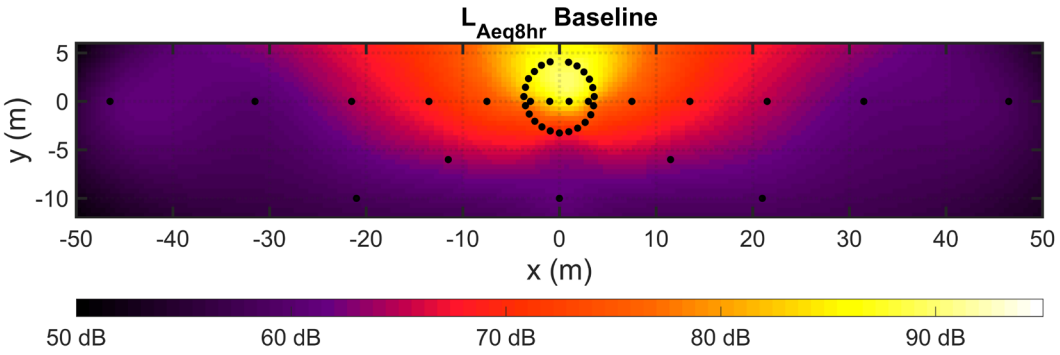

Figure 5-6. Baseline interpolation model of the 8-hr A-weighted equivalent level using all data points, Cartesian interpolation, and ghost points in map corners. Black dots represent microphone locations.

5.4 Spherical Spreading Predictions

In an ideal situation, a smaller number of microphones can be used to gather data that can be extended to the larger range. One of the potential decay rates for plotting is spherical. With every doubling of distance, peak levels should fall by 6-dB in all directions. With this knowledge, one could use only a polar arc of microphones to determine peak levels as a function of angle, and extrapolate outward to create an accurate interpolation. For peak levels, this is a very simple approach. With equivalent levels, the ground reflections could play a more important role. This is a subject for future work not covered in the depth is deserves in this thesis. The Quantico data set allows for comparisons of this approach and the predicted baseline model.

Data points along the arc can be used as references in spherical decay in the radial direction. For the map created, data was extrapolated to 46.5 m before then creating an interpolation map. The results for this interpolation are shown in Figure 5-7. Microphone locations are highlighted by the black dots on the map. Comparing with the baseline there are already noticeable

differences, particularly behind the shooter. The decay rate is much faster in the negative y-direction. Overall, the plot looks reasonable, but how does it compare to the baseline?

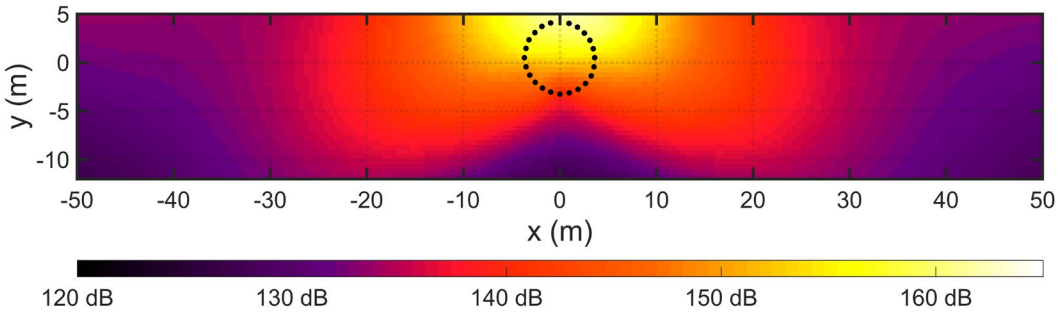

Figure 5-7. Peak level interpolation generated using data from the polar arc and extrapolating using a spherical spreading prediction. Microphone locations are shown as black dots.

By taking the difference between spherical spreading generated interpolations and the baseline, one can more clearly see the effects and limitations of spherical spreading as a means for map creation. This difference is shown in Figure 5-8. The spherical spreading prediction tends to struggle with predictions beyond the arc, often reaching up to and beyond 3 dB error. In the rear, this is likely due to effects of shielding. Corners are also potentially limited by azimuthal decay along the arc. The source is not omnidirectional.

This error is much greater than the 1 dB shot-to-shot deviation, and 3 dB again, is associated with an operational doubling or halving of rounds as outlined by the Hearing Conservation Program[24]. Effects are particularly unpredictable behind and to the left of the shooter. If one was truly limited in available microphone capabilities, this is a useable approach. However, it is not recommended compared to the baseline microphone spread.

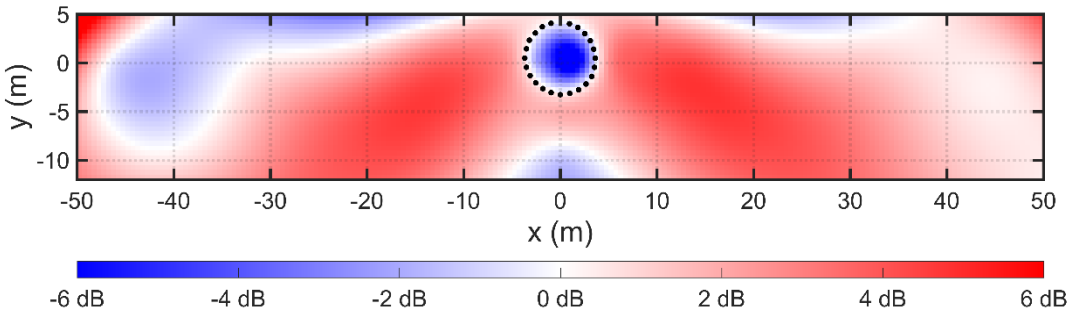

Figure 5-8. Difference between the baseline's and spherical spreading prediction's generated interpolations. Negative error represents a underprediction by the less complete data set.

While the comparison map shows a visual representation of the error, one can also look at error directly at measured data points and their surrounding areas. These results are shown in Table 5-1 for select microphone locations. An extended table for all missing data points from the baseline is shown in the appendix. While certain predicted points match up within 1-dB of the recorded data points, the spherical spreading tends to overpredict, as a whole. This means that the predicted level is slightly higher than the baseline level at that location. By only using four points at the corner, the interaction is different than creating ghost points inside the perimeter at 46.5 m. The predictions are typically below 2 dB, but could be further improved. For safety operations, this is not the worst case, as covering for overpredicted levels is safer in terms of exposure.

In terms of physical level predictions, spherical spreading tends to be up to 3-dB off, most likely due to some nonlinear aspects of small-firearms noise, or potentially due to ground reflections. The initial wave could merge with the reflection and increase the peak level, while not necessarily increasing the equivalent level. Inside of the arc, predictions are even worse, which due to the impulse nature of the source, is understandable. However, even as a means for predictions along the range, it is not recommended to use this approach.

TABLE 5-1. Error between the difference of the interpolation of spherical spreading predicted from peak levels measured at the arc versus the baseline. Errors are shown at known microphone locations and their surrounding areas. Extended table including all locations shown in appendix.

Microphone X-Location (m)	Microphone Y-Location (m)	Microphone r-location (m)	Microphone θ-location (degrees)	L_{pk} Error at Microphone Location (dB)	Average L_{pk} Error in 2m x 2m Area (dB)
-46.50	0.00	46.50	90	-0.51	-0.18
-31.50	0.00	31.50	90	0.24	0.15
-11.50	-6.00	13	77	4.16	4.10
-21.50	0.00	21.50	90	1.48	1.44
-13.50	0.00	13.50	90	3.58	3.43
-7.50	0.00	7.50	90	3.28	3.18
-1.00	0.00	1.00	90	-5.34	-4.66
1.00	0.00	1.00	-90	-8.84	-5.75
7.50	0.00	7.50	-90	3.83	3.81
13.50	0.00	13.50	-90	-4.29	4.13
21.50	0.00	21.50	-90	2.39	2.34
0.00	-10.00	10.00	180	-1.26	-0.94
31.50	0.00	31.50	-90	1.28	1.23
46.50	0.00	46.50	-90	0.79	0.90
11.50	-6.00	13	77	3.96	3.95
3.00	0.00	3.00	-90	-2.11	-1.72

5.5 Leave-one-out

Interpolation can cause errors due to computational limitations. Whether it is from minimal variables or interpolation type, Cartesian-type interpolation can lead to some error. In order to determine potential errors due to this interpolation, as well as to see the impact each measurement location has on the baseline, a leave-one-out analysis can be performed. Leave-one-out are often used in machine learning codes to test classification algorithms[25,26]. While this is not a machine learning process, the idea is the same.

Leave-one-out is defined to be removing one data point (location) from the baseline data set, and comparing the difference of the generated interpolations. In order to better understand the

effects, differences between the baseline and the leave-one-out generated interpolations are calculated at the point of interest, and in square areas of increasing size surrounding the location. Some of these differences are shown in Table 5-2, while complete results for the right-handed standing shooter are shown in the appendix.

TABLE 5-2. Peak level interpolation errors caused by removing one individual microphone at a time. This is dubbed a leave-one-out approach. Difference errors between leave-one-out and baseline interpolations are shown at known microphone locations and their surrounding areas. Extended table including all locations shown in appendix.

Microphone X-Location (m)	Microphone Y-Location (m)	Microphone r-location (m)	Microphone θ-location (degrees)	L_{pk} Error at Microphone Location (dB)	Average L_{pk} Error in 2m x 2m Area (dB)
-46.50	0.00	46.50	90	-4.86	-4.60
-11.50	-6.00	13	77	-0.16	-0.15
-21.50	0.00	21.50	90	0.08	0.08
-1.00	0.00	1.00	90	-0.99	-0.47
1.00	0.00	1.00	-90	-3.15	-1.51
0.00	-10.00	10.00	180	-11.08	-10.64
31.50	0.00	31.50	-90	0.93	0.90
46.50	0.00	46.50	-90	-1.60	-1.51
11.50	-6.00	13	-77	0.19	0.18
0.00	-3.67	3.67	180	1.62	0.50
-3.12	-1.30	3.67	120	1.98	0.59
-3.51	-0.44	3.67	105	-1.09	-0.24
3.11	2.29	3.67	-60	0.71	0.23
3.45	1.43	3.67	-75	-0.34	-0.08
-3.00	0.00	3.00	90	-0.59	-0.09
3.00	0.00	3.00	-90	-0.18	-0.03

Certain microphones tend to be much more important for limiting error than others. For many locations, particularly along the arc, removing a singular data point only amounts to 0.5 dB error, which falls within the shot-to-shot deviation. This, coupled with the results of polar arc limitations would help reduce the number of microphones needed. Microphones at large

distances away, particularly in the negative x-direction started to see large errors when removed. These distances typically had larger shot-to-shot deviations, however, seem to be more relevant in creating baseline results.

The largest source for error in the leave-one-out analysis proved to be from microphones directly behind the source. While not shown here, this is consistent even for the shooter stand, where less shielding is present. This means that the gun itself plays some role in shielding. By removing the microphone 10 meters behind the shooter, interpolation errors reached up to 10 dB at location. This is also partially due to under sampling in the rear, and shows the value of multiple data points behind the shooter. Errors in the surrounding areas were also much higher. A plot for this leave-one-out interpolation in particular is shown in Figure 5-9. The figure highlights the impact of the radial decay in the rear direction. Even without a comparison map, the effect of removing this data point on the interpolation is clear.

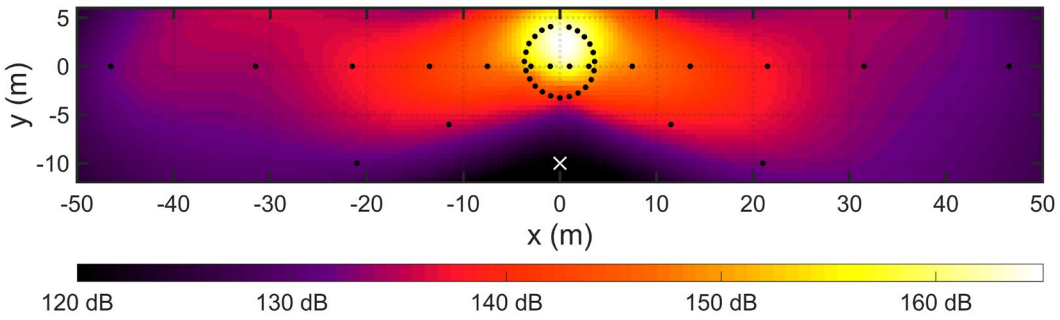

Figure 5-9. Peak level (dB) interpolation map created from all data except for the level recorded 10 meters behind the origin. This location is shown as a white X on the plot.

A comparison map between the baseline and the same left-out point further highlights the issues with the data point removal. Figure 5-10 shows that there is a large underprediction behind the shooter without the data point. As mentioned in the spherical spreading analysis, overpredictions are not the worst-case scenario in exposure predictions. While they might not be

as accurate, they will protect shooters from overexposure. This is also a location in which a drill instructor or onlookers would often stand, and therefore has significant relevance in predictions. Of all microphone locations, it seems that microphones behind the shooter tend to be most impactful in baseline interpolations. Certain mics along the arc or perhaps the firing line could be considered for removal, but microphones behind the shooter need to take priority.

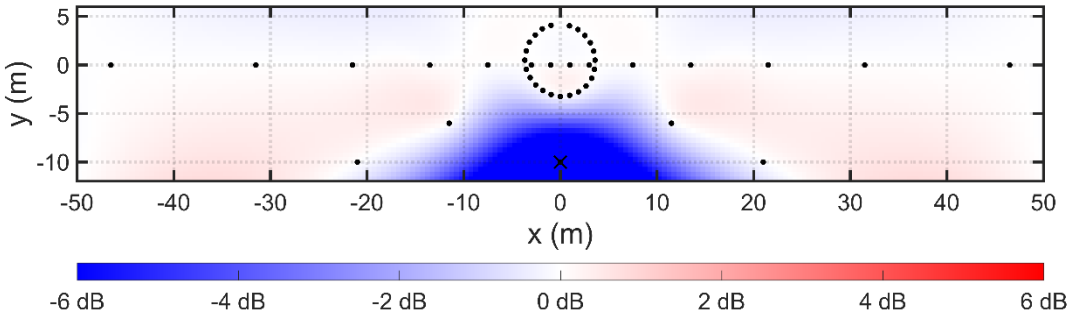

Figure 5-10. Difference between the baseline and leave-one-out generated interpolations. Data from 10 meters behind the shooter was removed. The black dot represents the data point removed. Negative error represents a underprediction by the less complete data set.

5.6 Symmetry

One last approach to limit required microphones for accurate measurement is to rely on a left-right symmetry between the data. By taking only the negative x-data points and reflecting them across the y-axis, interpolated level maps can be created with half of the required measurement points. These reflections also include anything along the y-axis, as microphones directly behind the shooter are inherently relevant. Following this approach for the right-handed standing shooter resulted in the plot shown in Figure 5-11. This plot is noticeably symmetric, but

from first glance seems to predict results well. Shielding in the rear is present and radial decay patterns seem reasonable.

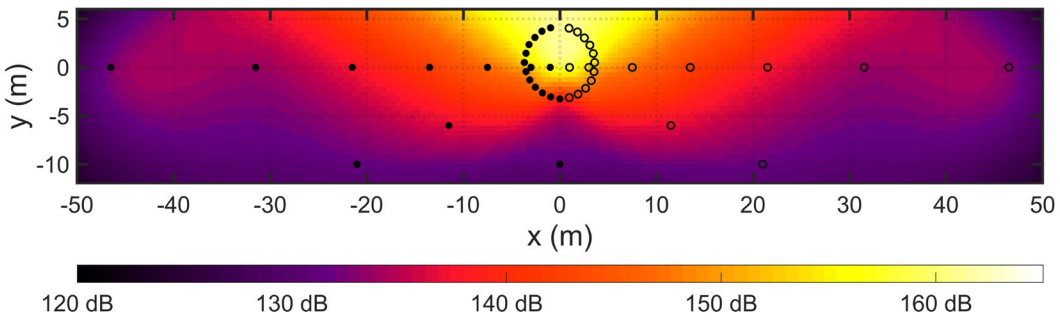

Figure 5-11. Peak level (dB) interpolation map created using a symmetrical assumption. Negative-x data was reflected across the y-axis and used to create the level map. Reflected points are shown as non-filled circles.

For this analysis, a comparison plot better highlights potential issues with a symmetrical source prediction. Taking the difference between the symmetric data and the baseline and plotting results in Figure 5-12. A symmetrical assumption performs well between the polar arc array and roughly up to 30 meters away from the origin. Difference errors mostly fall below 1 dB, well within the shot-to-shot deviation. The averaged absolute dB-difference was calculated to be 1.03 dB. The symmetrical assumption, however, tends to see issues at large radial distances and inside of the polar arc (within 3 meters). When using the positive x-data, errors are flipped. Where there was an overprediction, there would be an underprediction.

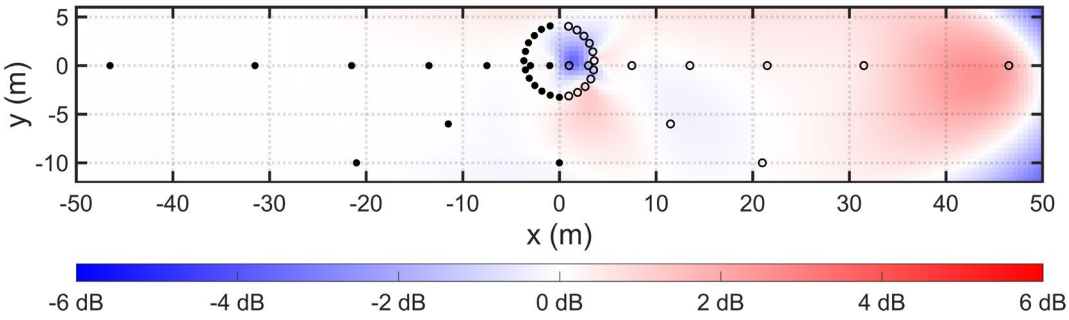

Figure 5-12. Difference between the symmetrical generated and baseline interpolations. Data from the negative x-data was reflected to the positive x-side side. Negative error represents a underprediction by the less complete data set.

For a smaller range, and potentially coupled with more interior data points, a symmetrical assumption is a viable approach to limit require measurement points. The baseline will always perform better, but perhaps microphones along the firing line can be moved to either behind the shooter, or in a location with less coverage. From an operational exposure perspective, it would be more appropriate to use data points to the left of the shooter, as an overprediction by the reflected data is safer than an underprediction. This is probably the best approach to make with limited microphones, as it extends the coverage much further than any other attempted simplication.

5.7 Best Practices

With the above analyses, a new interpolation map can be created with limited numbers of microphones. With the principles applied, one can create a map with minimal error with only half of the microphones used in the baseline. This process could have been optimized, but for the purposes of this thesis, choices were made based on analytical results. The first choice made was to reduce the number of microphones selected along the firing line. Then, using symmetry behind and to the left of shooter, microphones could be mirrored across the firing direction.

Finally, a reduced number of microphones from the arc were used, while maintaining finer resolution in the rear The microphones selected for this recommendation are shown in Figure 5-13.

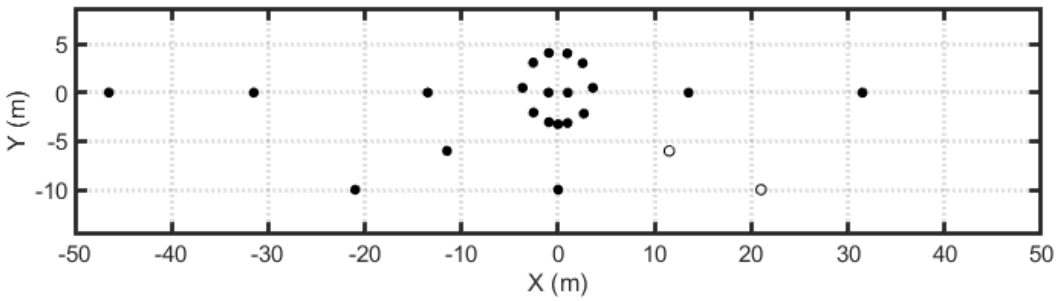

Figure 5-13. Microphone locations chosen to achieve acceptable interpolation results with minimal data points. The two empty circles represent data achieved by reflecting three points from the negative y-axis.

Creating a comparison map shown in Figure 5-14 results in minimal error between the two interpolations. At large distances, as one might expect, there is slightly more error; however, the interpolation performs well overall. By removing some microphones along the firing line to the right of the shooter, oscillatory behavior is created. There is still an overall decay, but it is not possible to say it will always over or under-predict on the side with fewer microphones. Nevertheless, this limited microphone set would perform well in exposure predictions and potential military firearms drill design.

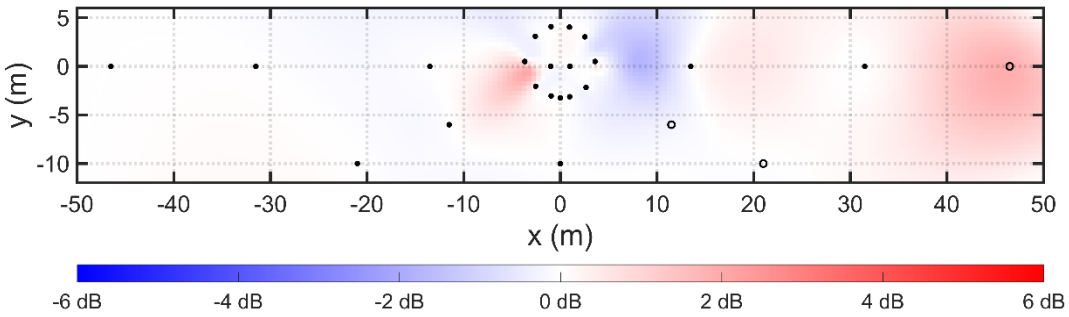

Figure 5-14. Difference between the baseline and the intuitive optimized peak level maps. Error is typically below 1 dB. Negative error represents a underprediction by the less complete data set.

Using the insights gained from analyses on the peak level, the same microphone selection can be used in equivalent level predictions. The results for this interpolation comparison are shown in Figure 5-15. Again, this interpolation from a minimal number of microphones performs well. While there is slightly more error in the far field, the error is typically below 2 dB. Again, more microphones will always give more accurate results, but this microphone selection allows for efficient data collection.

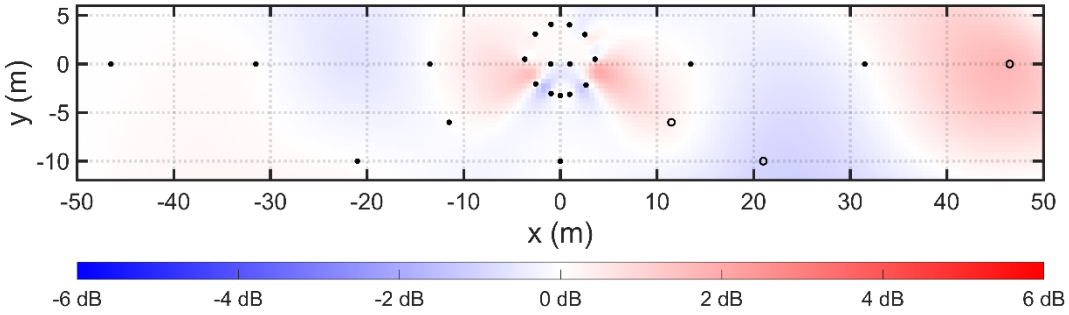

Figure 5-15. Difference between the baseline and the intuitive optimized level maps for the 8-hour A-weighted equivalent level (L_{Aeq8hr}). Error is typically below 1 dB. Negative error represents a underprediction by the less complete data set.

Chapter 6

Conclusions

This chapter will briefly go over main points made in the thesis, as well as qualify the analyses made. At the end, ideas and sources for future work are discussed.

6.1 Results

The first thing shown in this thesis is that the data recorded at Marine Base Quantico of the M16A4 rifle are valid. Trends are consistent with previously taken small firearms measurements and efforts were made to ensure accurate recordings. While the data are good, there is some inherent uncertainty within the data. Looking at the standard deviations between a 10 shot volley, deviations are roughly 1 dB for peak levels, while reaching up to 1.5 dB for the A-weight 8-hour equivalent level. These deviations serve as a good baseline for the error analyses.

Looking at the waveforms themselves, there are significant differences between standing, kneeling, and prone shooter events, as well as at recording locations of mirroring heights. As the recording height lowered, the sharpness of the waveform decreased, and the overall levels decreased as well at a similar distance. There was roughly a 3 dB spread between each configuration, with no trend. A conservative 3 dB blanket addition could be made where multiple configurations could not be measured. While the preliminary results were discussed, in depth analyses of these height differences are left for future studies.

In order to determine the best practices for creating predictive level maps, different error analyses were performed. Before diving into these analyses, radial decay was first examined. It was shown that although spherical spreading was a conservative estimate, it tended to overpredict levels in the far field by up to 4 dB at 50 m. A conservative estimate functions

adequately for exposure predictions, as it would more-easily protect small firearms users. The decay rate, however, definitely exceeds the typical spherical spreading predictions.

Two main methods were investigated for interpolation in level maps predictions: Cartesian and polar. The polar interpolation saw issues with oscillatory behavior, while the Cartesian interpolation ran into non-physical behavior at map extremities. The levels would tend to rise, and predict an increase in level at distance. By using a conservative spherical spreading model, ghost points were employed to overcome these issues. Using Cartesian interpolation and ghost points, a baseline prediction map was generated.

The main error analyses were performed to determine microphone location relevance for future small firearms measurements. First, a level map was made using a spherical spreading prediction from the central arc extending out to 46.5 m. This approach struggled in the rear, likely due to rifle and shooter shielding effects. Second, using a reflective symmetry across the y-axis (or firing direction), one could generate level maps with errors typically below 3 dB on the reflected side. Lastly, using a leave-one-out type analysis showed the importance of microphones directly behind the shooter. In the Quantico data, sample points directly behind the shooter were limited, and led to up to 10 dB of error when left out.

Finally, an overall recommendation was given on how to approach future small firearms measurements but with minimal microphones or sampling locations. Using a combination of symmetry and selective microphone placement, level maps were created with errors on average less than 1 dB compared to the baseline. The main takeaway from this thesis is the ability to produce accurate level maps for the M16A4 rifle, and give a framework for any future small firearms measurements

The other big insight gained is that even a rich dataset from Quantico can lead to more questions than it can necessarily answer. It seems that a blast wave decay prediction could fit for radial decay, but there is not necessarily a lot of data sets to compare back to for small firearms. This also only speaks to the peak level, and does not begin to cover equivalent levels. Even within the Quantico data set, there are minimal points with which to truly understand the decay rate. There seems to be something contributing to a decay rate faster than spherical spreading predicts, but a definitive answer cannot yet be given. More data would need to be taken in order to definitively accept a specific decay rate.

Requirements given in the ANSI S12.7[11] are accurate in requiring multiple configurations for a complete test, such as varying microphone and shooter heights. Overall, the thesis provides better understanding of how the M16A4 rifle produces sound in an outdoor range, and can better predict what levels will be seen on the firing range with minimal errors. Future tests can now be optimized and avoid superfluous microphone placement.

6.2 Qualifying Arguments and Future Work

One of the big issues with the data set is a lack of precise consistency. Between each configuration there was a potential shooter swap. With this shooter swap comes height change, potential change in the x-y plane, and overall posture change. Getting a birds-eye view would be optimal in the future, along with an easy way to see exactly where the muzzle is located for each configuration. One discussed idea is to lay a checkerboard map below the shooter, with defined distances between each square. This, coupled with a birds-eye view, would guarantee an accurate source location assessment.

In the end, no data set is ever perfect, but the efforts of this thesis show approaches to take when making measurements. That said, there are several analyses still to be done on the data set.

There is still much to be learned about the differences, if any, between right-handed and left-handed shooters. Beamforming can be used to better understand the geometry of the M16A4 rifle. One can also look into the interaction between direct and reflected waves. Using distances from source to receiver, predictions could be made using basic simulated waveforms. While the waveforms would be difficult to fit perfectly, basic models can be used to predict rough waveform shapes throughout the range. The basic model could then be adapted to an indoor range environment, where there are many more reflective surfaces. This will then provide more framework for future measurements, whether indoors or outdoors.

6.3 Significance

Although there is still much to be done, and many more analyses ready for small firearms, this thesis makes significant progress into future measurement design. Being able to have a guide for future measurements, as well as an easy way to calculate levels around the field will greatly help in drill design for the military, as well as understanding potential ways to limit risk for all firearms users. At the time of writing this thesis, one more extensive measurement has been made of the AR-15 Rifle. This data will help potentially fill in some gaps from the Quantico measurement. This thesis provides some framework for modeling predictions and can hopefully be used as a source for any future small firearms level maps predictions.

References

[1] R. D. Rasband, A. T. Wall, K. L. Gee, S. H. Swift, C. M. Wagner, W. J. Murphy, C. A. Kardous, “Impulse Noise Measurements of M16 Rifles at Quantico Marine Base,” POMA (2018).

[2] L. Marshall, J. A. Lapsley Miller, L. M. Heller, K. S. Wolgemuth, L. M. Hughers, S. D. Smith, and R. D. Kopke, “Detecting incipient inner-ear damage from impulse noise with otoacoustic emissions,” J. Acoust. Soc. Am. **125**(2), 995-1013 (2008).

[3] K. Yankaskas, “Prelude: noise-induced tinnitus and hearing loss in the military,” Hear Res. (2013).

[4] Recreational Firearm Noise Exposure. http://www.asha.org/public/hearing/Recreational-Firearm-Noise-Exposure/

[5] R. R. A. Coles, G. A. Garinther, G. C. Hodge, and C. R. Rice, “Criteria for Assessing Hearing Damage Risk from Impulse-Noise Exposure,” U.S. Army Technical Memorandum 13-67 (1967).

[6] National Institute for Occupational Safety and Health, “Criteria for a Recommended Noise Exposure, Occupational Noise Exposure,” U.S. Department of Health and Human Services (1998).

[7] Department of Defense Instruction, “Hearing Conservation Program (HCP),” DoDI Number 6055.12, (December 3, 2010).

[8] W. J. Murphy, G. Flamme, E. L. Zechmann, C. Dektas, D. K. Meinke, M. Stewart, J. E. Lankford, and D. Finan, “Noise exposure profiles for small-caliber firearms from 1.5 to 6 meters,” J. Acoust. Soc. Am. **132**(3), 1905 (2012).

[9] Shakti K. Davis, Paul T. Calamia, William J. Murphy & Christopher J. Smalt (2019): In-ear and on-body measurements of impulse-noise exposure, International Journal of Audiology, DOI: 10.1080/14992027.2018.1534012

[10] Miltary Standard MIL-STD-1474E, Design Criteria Standard Noise Limits, (DOD 15 April 2015).

[11] ANSI S12.7-1986 (R2015), “American National Standard Methods for Measurement of Impulse Noise,” American National Standards Institute (1986).

[12] W. L. Acton, and M. R. Forrest, “Hearing Hazard from Small-Bore Weapons,” J. Acoust. Soc. Am. **44**(3), 817-818 (1968).

[13] P. G. Weissler, and M. T. Kobal, “Noise of police firearms,” J. Acoust. Soc. Am. **56**(5), 1515-1522 (1974)

[14] P. Rasmussen, G. Flamme, M. Stewart, D. Meinke, and J. Lanford “Measuring Recreational Firearm Noise,” SandV August, (2008).

[15] S. D. Beck, H. Nakasone, and K. W. Marr, “Variations in recorded acoustic gunshot waveforms generated by small firearms,” J. Acoust. Soc. Am. **129**(4), 1748-1759 (2011).

[16] T.K. Routh and R.C. Maher, "Recording anechoic gunshot waveforms of several firearms at 500 kilohertz sampling rate," Proc. Mtgs. Acoust. (POMA) 26, 030001 (2016).

[17] A. T. Wall, C. M. Wagner, R. D. Rasband, K. L. Gee, "Cumulative noise exposure model for outdoor shooting ranges," J. Acoust. Soc. Am. **146**(5) (2019).

[18] C. M. Wakefield, Wakefield Acoustics Ltd., "The Effects of Firing Patterns, Meteorology and Terrain on Community Noise Exposures from a Military Rifle Range" (1995)

[19] P. Rasmussen, "An improved Method for 3D Vector Intensity Measurements: The G.R.A.S. Intensity Sphere," G.R.A.S. Whitepaper, March 2016, https://www.grasacoustics.com/files/m/a/Intensity_Sphere.pdf

[20] M. B. Muhlestein, K. L. Gee, and J. H. Macedone, "Educational demonstration of a spherically propagating acoustic shock," J. Acoust. Soc. Am. **131**, 2422–2430 (2012).

[21] S. M. Young, K. L. Gee, T. B. Neilsen, and K. M. Leete, "Outdoor measurements of spherical acoustic shock decay," J. Acoust. Soc. Am. **138**, EL305 (2015).

[22] ANSI S2.20-1983: American National Standard for Estimating Airblast Characteristics for Single Point Explosions in Air (Acoustical Society of America, Melville, NY, 2006).

[23] Jamal, RegularizeData3D, MATLAB Central File Exchange (https://www.mathworks.com/matlabcentral/fileexchange/46223-regularizedata3d). Retrieved June 21, 2021.

[24] United States Department of Defense Instruction Number 6055.12, "Hearing Conservation Program (HCP)," Office of the Under Secretary of Defense for Acquisition, Technology, and Logistics (December 3, 2010)

[25] T. Wong, "Performance evaluation of classification algorithms by k-fold and leave-one-out cross validation," Pattern Recognition, Vol. 48, Issue 9 (2015).

[26] K. Pederson, M. K. Transtrum, K.L. Gee, B. A. Butler, M. M. James, A. R. Salton, "Machine learning-based ensemble model predictions of outdoor ambient sound levels," Proc. Mtgs. Acoust. **35**, 022002 (2018).

Appendix A

This appendix attempts to extend tables found in Chapter 5. It also contains a table comparing values predicted using a spherical spreading model with those at measured locations. This provides the further information in case one wanted more specific examples of errors at various locations for different approaches.

Table 5-1 Extended. Difference between recorded levels and levels acquired through interpolation from the nearest two microphones along the microphone arc. Results are shown for both peak levels and 8-hr A-weighted equivalent levels.

Angle	-75°	-60°	-45°	-30°	-15°	0°	15°	30°	45°	60°	75°	90°
L_{pk} Error (dB)	0.6	-0.1	0.3	0.3	0.4	-	0.4	0.2	0.3	0.5	0.2	-0.1
L_{Aeq8hr} Error (dB)	0.4	0.1	1.2	-0.9	0.5	-	0.8	0	0	0.5	0.4	0.3
Angle	105°	120°	135°	150°	165°	±180°	-165°	-150°	-135°	-120°	-105°	-90°
L_{pk} Error (dB)	-0.4	0.1	-0.3	-0.3	1.6	-2.1	-1.8	0.6	-0.2	0.4	-0.5	0
L_{Aeq8hr} Error (dB)	-0.4	-0.3	-1.8	1	.5	-1.9	-0.8	-0.4	0.7	-0.1	-0.5	0

Table 5-2 Extended. Peak level interpolation errors caused by removing one individual microphone at a time. This is dubbed a leave-one-out approach. Difference errors between baseline and leave-one-out interpolations are shown at known microphone locations and their surrounding areas.

Microphone X-Location (m)	Microphone Y-Location (m)	L_{pk} Error at Microphone Location (dB)	Average L_{pk} Error in 2m x 2m Area (dB)	Average L_{pk} Error in 5m x 5m Area (dB)	Average L_{pk} Error in 10m x 10m Area (dB)
-46.50	0.00	4.86	4.60	3.20	1.70
-31.50	0.00	-2.22	-2.15	-1.94	-1.37
-21.00	-10.00	1.59	1.56	1.55	1.28
-11.50	-6.00	0.16	0.15	0.11	0.05
-21.50	0.00	-0.08	-0.08	-0.06	-0.04
-13.50	0.00	-0.81	-0.73	-0.51	-0.26
-7.50	0.00	1.38	1.14	0.62	0.22
-1.00	0.00	0.99	0.47	0.04	-0.08
1.00	0.00	3.15	1.51	0.20	-0.24
7.50	0.00	1.61	1.33	0.62	0.26
13.50	0.00	-0.77	-0.70	-0.43	-0.25
21.50	0.00	-0.52	-0.49	-0.35	-0.23
0.00	-10.00	11.08	10.64	9.16	7.78
31.50	0.00	-0.93	-0.90	-0.73	-0.57
46.50	0.00	1.60	1.51	1.26	0.56
11.50	-6.00	-0.19	-0.18	-0.13	-0.06
21.00	-10.00	2.40	2.36	2.02	1.93
0.00	-3.25	-1.62	-0.50	-0.17	-0.03
-0.95	-3.04	0.78	0.19	0.06	0.02
-1.81	-2.63	-0.01	0.00	0.00	0.00
-2.55	-2.05	0.67	0.16	0.07	0.02
-3.12	-1.30	-1.98	-0.59	-0.21	-0.04
-3.51	-0.44	1.09	0.24	0.07	-0.01
-3.68	0.50	-0.61	-0.16	-0.04	0.01
-3.51	1.46	0.54	0.11	0.01	-0.03
-3.20	2.35	-0.62	-0.22	-0.16	-0.12
-2.59	3.09	0.31	0.07	0.01	-0.01
-1.86	3.73	-0.15	-0.06	-0.05	-0.04
-0.96	4.08	0.00	0.00	0.00	0.00
0.95	4.04	-0.22	-0.09	-0.05	-0.05
1.82	3.65	-0.01	0.00	0.00	0.00

2.54	3.04	0.37	0.09	0.02	0.01
3.11	2.29	-0.71	-0.23	-0.08	-0.08
3.45	1.43	0.34	0.08	0.01	-0.01
3.60	0.50	-0.01	0.00	0.00	0.00
3.53	-0.45	-0.30	-0.06	-0.02	0.00
3.25	-1.38	-0.22	-0.07	-0.02	0.00
2.66	-2.16	0.27	0.08	0.02	0.01
1.88	-2.76	-0.14	-0.04	-0.01	-0.01
0.97	-3.12	0.25	0.06	0.01	0.00
-3.00	0.00	0.59	0.09	-0.04	-0.03
3.00	0.00	0.18	0.03	-0.01	-0.01

Table A-1 Error between the difference of the entire data interpolation versus using a spherical spreading prediction from peak levels measured at the arc. Errors are shown at known microphone locations and their surrounding areas.

Microphone X-Location (m)	Microphone Y-Location (m)	L_{pk} Error at Microphone Location (dB)	Average L_{pk} Error in 2m x 2m Area (dB)	Average L_{pk} Error in 5m x 5m Area (dB)	Average L_{pk} Error in 10m x 10m Area (dB)
-46.50	0.00	0.51	0.18	-1.02	-3.41
-31.50	0.00	-0.24	-0.15	0.15	0.58
-21.00	-10.00	-4.12	-4.11	-3.94	-3.27
-11.50	-6.00	-4.16	-4.10	-3.76	-2.44
-21.50	0.00	-1.48	-1.44	-1.15	-0.07
-13.50	0.00	-3.58	-3.43	-2.72	-0.74
-7.50	0.00	-3.28	-3.18	-2.38	-0.56
-1.00	0.00	5.34	4.66	0.76	-0.68
1.00	0.00	8.84	5.75	0.64	-0.74
7.50	0.00	-3.83	-3.81	-2.91	-0.96
13.50	0.00	-4.29	-4.13	-3.38	-1.40
21.50	0.00	-2.39	-2.34	-2.03	-0.94
0.00	-10.00	1.26	0.94	0.21	-0.41
31.50	0.00	-1.28	-1.23	-1.06	-0.65
46.50	0.00	-0.79	-0.90	-1.32	-2.15
11.50	-6.00	-3.96	-3.95	-3.75	-2.59
21.00	-10.00	-4.15	-4.14	-3.99	-3.36
-3.00	0.00	1.63	1.02	0.12	-0.62
3.00	0.00	2.11	1.72	-0.08	-0.79

Appendix B

The plots shown here merely supplement plots shown in Chapter 5. There are many more plots that could be made and shown, but these show some results for the left-handed shooter as well as some other examples of leave-one-out analyses. More can be made using the relevant codes.

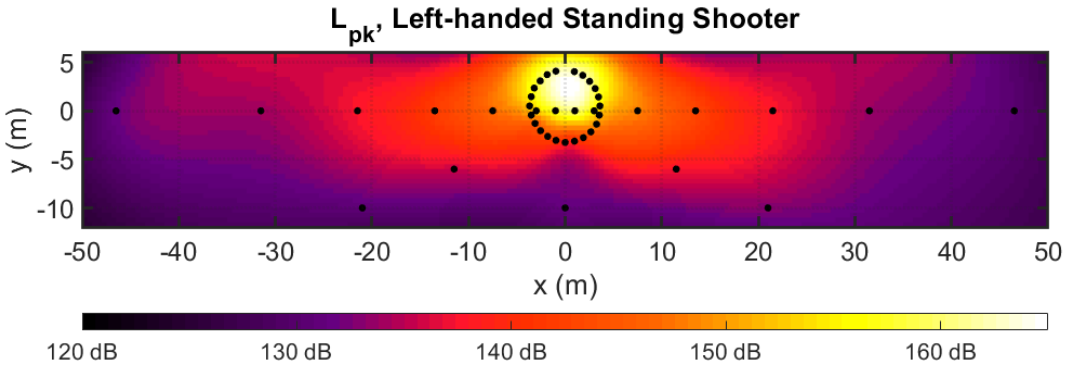

Figure B-1. Peak level map with Cartesian interpolation with ghost points for a standing, left-handed shooter.

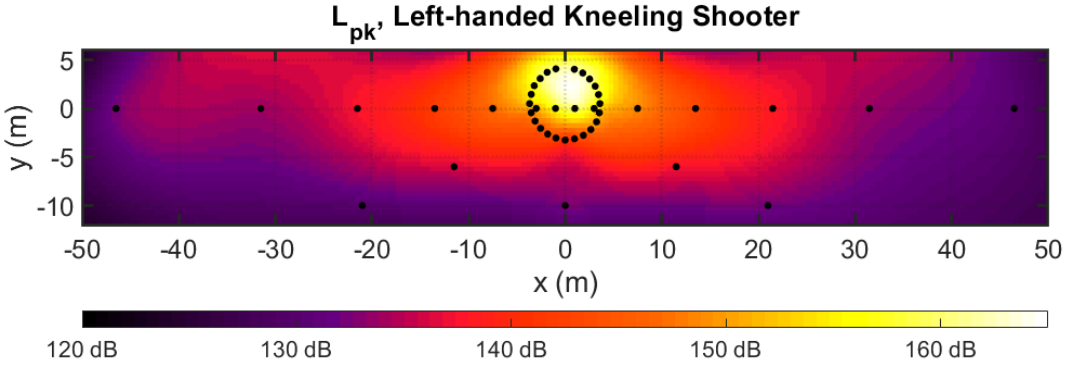

Figure B-2. Peak level map with Cartesian interpolation with ghost points for a kneeling, left-handed shooter. Microphones used for interpolation are at a standing height.

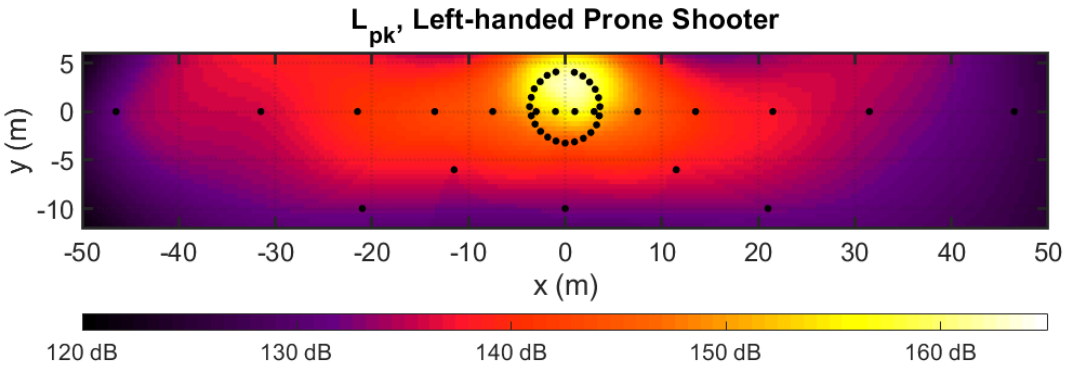

Figure B-3. Peak level map with Cartesian interpolation with ghost points for a prone, left-handed shooter. Microphones used for interpolation are at a standing height.

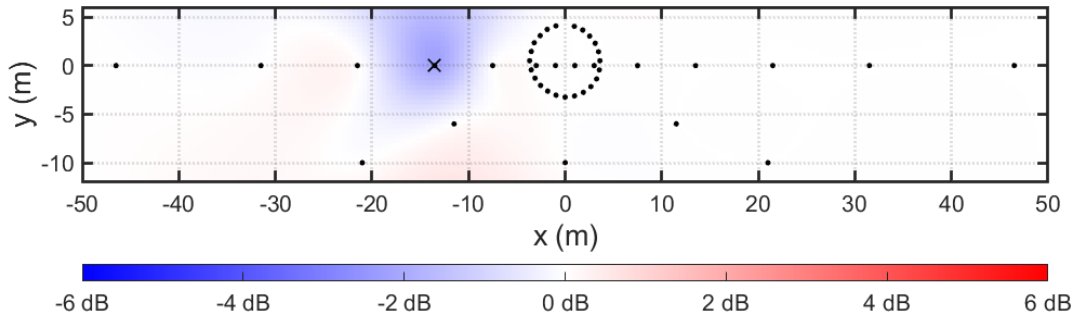

Figure B-4. Leave-one-out comparison map for microphone located at x = -7.5 m, y = 0 m. This microphone is much less relevant than a microphone behind the shooter.

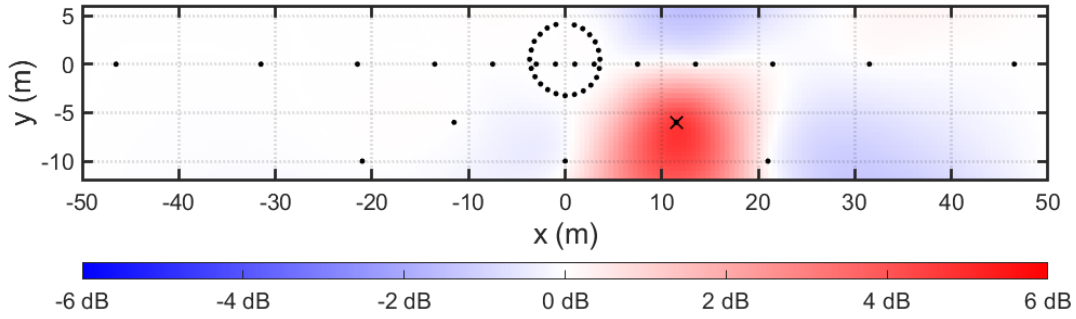

Figure B-5. Leave-one-out comparison map for microphone located at x = 11.5 m, y = -6 m. This microphone is less relevant than a microphone directly behind the shooter, but is still relevant in predictions. This could also be an instructor position, and is a valuable spot for a microphone.